Chapter 6
Neurons, Connections, and Microcircuits of the Inferior Colliculus

Tetsufumi Ito and Manuel S. Malmierca

Abstract In this chapter, the neural circuitry of the inferior colliculus (IC) is described at a cellular level. The IC is subdivided into the central nucleus (ICC) and surrounding cortices that receive specific combinations of inputs and generate diverse outputs. Neuronal types in the IC can be distinguished by their dendritic arborization patterns, neurochemical profiles, and physiological properties. Based on these properties, neuronal types organizing the ICC appear to be different from those organizing the IC cortex. The IC receives ascending inputs from the cochlear nuclei, superior olivary complex, and nuclei of the lateral lemniscus, and the IC receives descending inputs from the auditory cortex and nonauditory inputs from various nuclei. Each input source forms terminal fields in particular zones of the IC. Massive commissural and local inputs are also present. One well-characterized cell type, the large GABAergic IC neuron, receives convergent input from all of these sources. The IC neurons project to the auditory thalamus as well as to lower brain stem nuclei. Anatomical and physiological features suggest that ICC acts as an auditory integration center, and IC cortex acts as a multimodal integration center and novelty detector. These data support the view that the lemniscal and nonlemniscal pathways emerge at the midbrain level.

T. Ito (✉)
Department of Anatomy, School of Medicine, Kanazawa Medical University, Uchinada, Ishikawa, Japan
e-mail: itot@kanazawa-med.ac.jp

M. S. Malmierca
Auditory Neuroscience Laboratory, Institute for Neuroscience of Castilla y León, University of Salamanca, Salamanca, Spain

Department of Cell Biology and Pathology, Faculty of Medicine, University of Salamanca, Salamanca, Spain

The Salamanca Institute for Biomedical Research (IBSAL), Salamanca, Spain
e-mail: msm@usal.es

D. L. Oliver et al. (eds.), *The Mammalian Auditory Pathways*,
Springer Handbook of Auditory Research 65,
https://doi.org/10.1007/978-3-319-71798-2_6

Keywords Ascending fibers · Commissural fibers · Descending fibers · GABA · Glutamate · Intrinsic membrane properties · Lemniscal auditory pathway · Local circuit · Neurotransmitter · Nonlemniscal auditory pathway · Sound-evoked activity · Synaptic domain

6.1 Introduction

The inferior colliculus (IC) is a midbrain auditory structure that receives inputs from virtually all lower brainstem auditory nuclei and sends information to the thalamus. In addition to the convergence of inputs from these nuclei, IC neurons, which can be subdivided into various types, interconnect with each other. This unique local circuitry allows the emergence of new coding strategies for auditory information. This chapter highlights the anatomical organization of the IC and its physiological correlates. For most of the chapter, the focus is on the differences between the core area (central nucleus, lemniscal pathway) and shell areas (IC cortex, nonlemniscal pathways). All abbreviations are explained in Table 6.1.

6.2 Cytoarchitecture of the Inferior Colliculus

Numerous cytoarchitectonic studies of the IC have accumulated over the past 50 years. These have focused on its organization in a variety of species, including nonmammalian clades. There is a general consensus that the IC consists of a central nucleus that is surrounded by collicular cortices. The main goal here is to provide the reader with a brief introduction as background for the discussion of the intrinsic organization of the IC. A detailed description of interspecies variations is outside the scope of this chapter and is described elsewhere (e.g., Covey and Carr 2005). Here, descriptions are focused on the IC of rats and mice for which there is now a great deal of molecular, electrophysiological, and behavioral data.

The IC is a large, oval-shaped structure located in the dorsocaudal midbrain. The left and right ICs are interconnected by a large, heavily myelinated commissure (the commissure of the IC, CoIC). The central nucleus of the IC (ICC) is surrounded by dorsal, lateral, and rostral cortices. In coronal sections at levels including the central nucleus, the dorsal cortex (ICD) and lateral cortex (ICL) are located dorsomedial and lateral to the central nucleus, respectively (Fig. 6.1) (Loftus et al. 2008). In more caudal sections, the central nucleus disappears and the dorsal and lateral cortices merge together (Faye-Lund and Osen 1985); this merged zone is called the caudal cortex (Morest and Oliver 1984). Rostral to the central nucleus, forming the rostromedial boundary of the IC is a region that, in rats, is now commonly referred to as the rostral cortex (ICR) (Malmierca et al. 2011). Together with the ICL, the ICR was included as a part of the external cortex by Faye-Lund and Osen (1985) in

Table 6.1 Abbreviations

A1	Primary auditory cortex
AC	Auditory cortex
CF	Characteristic frequency
CN	Cochlear nucleus
CoIC	Commissure of the inferior colliculus
DCN	Dorsal cochlear nucleus
DNLL	Dorsal nucleus of the lateral lemniscus
EPSP	Excitatory postsynaptic potential
F	Flat or disc-shaped neurons in ICC
FD-BDA	Fluorescein dextran and biotinylated dextran amine
FM	Frequency modulation
GABAergic	Gamma-aminobutyric acid neurotransmitter
GAD	Glutamic acid decarboxylase
GFP	Green fluorescent protein
IC	Inferior colliculus
ICC	Central nucleus of the IC
ICD	Dorsal cortex of the IC
ICL	Lateral cortex of the IC
ICR	Rostral cortex of the IC
INLL	Intermediate nucleus of the lateral lemniscus
IPSP	Inhibitory postsynaptic potential
ITD	Interaural time difference
LF	Less flat or stellate neurons in ICC
LG	Large GABAergic
LSO	Lateral superior olive
MGB	Medial geniculate body
MGD	Dorsal division of the MGB
MGM	Medial division of the MGB
MGV	Ventral division of the MGB
MSO	Medial superior olive
NLL	Nucleus of the lateral lemniscus
SG	Small GABAergic
SOC	Superior olivary complex
SSA	Stimulus-specific adaptation
VCN	Ventral cochlear nucleus
VGLUT	Vesicular glutamate transporter
VLN	Ventrolateral nucleus of the IC
VNLL	Ventral NLL

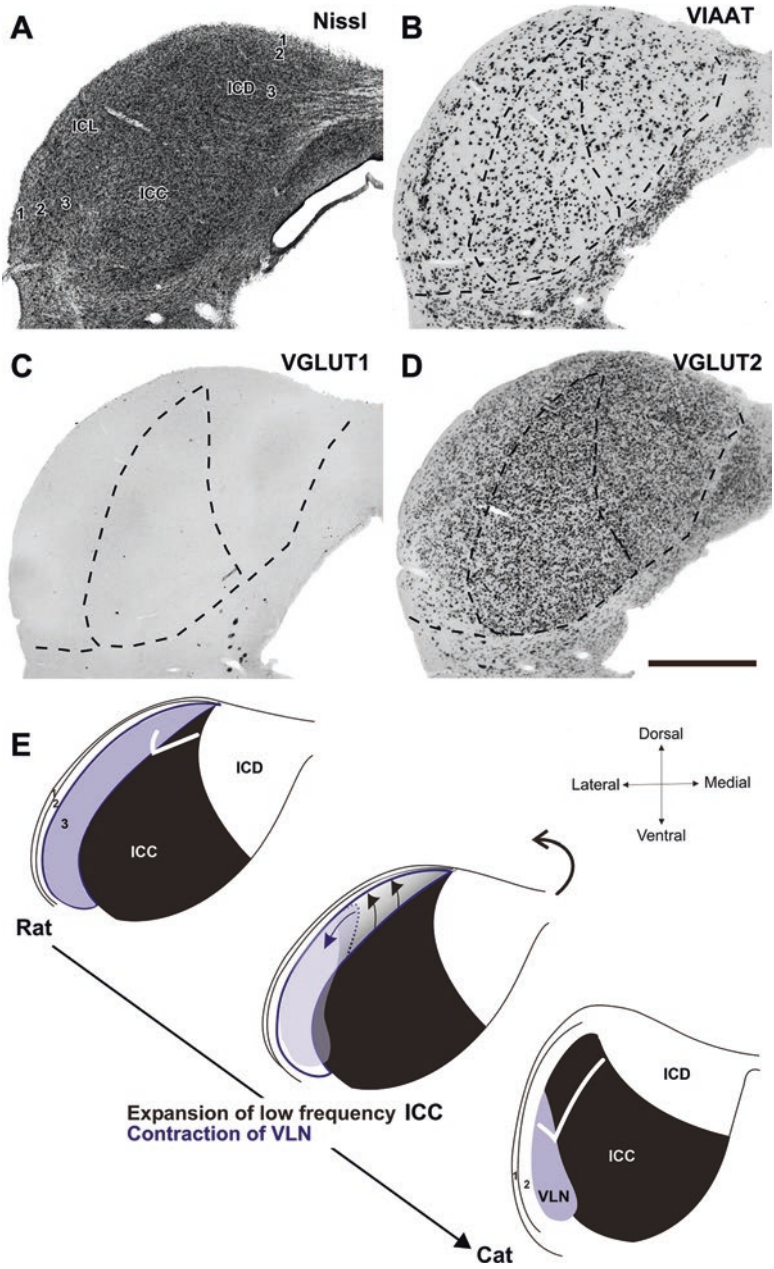

Fig. 6.1 Cytoarchitecture of the inferior colliculus (IC). **(A–D)** Labeling of cell bodies in the rat IC with several markers. Serial IC sections were processed for each staining. **(A)** Three subdivisions and layers in the cortices are discriminated with Nissl staining: central nucleus, *ICC*; dorsal cortex, *ICD*; lateral cortex, *ICL*. Layers *1, 2, 3* are also illustrated. **(B)** In the IC, VIAAT-positive neurons represent the GABAergic phenotype. Density of VIAAT-positive neurons is higher in the

their study of subdivisions in the rat, but now the ICR is known to have cell types and physiological properties different from those of the lateral (external) cortex. At the ventral extreme of the IC, a rostral extension of the central nucleus is sometimes referred to as the *rostral pole nucleus*. More laterally, layer 1 of the lateral cortex thickens and is continuous with the brachium of the IC.

6.2.1 Central Nucleus

The ICC is defined by the presence of fibrodendritic laminae that are composed of bundles of axons and dendritic arbors (Oliver and Morest 1984). The thickness of one lamina is about 50–70 μm (Malmierca et al. 1993). Within the laminae, numerous flat cell bodies are identified by Nissl staining and in situ hybridization (Fig. 6.1A, D) and correspond to disc-shaped or flat neurons. The main origin of axons in the fibrodendritic laminae is lemniscal, consisting of ascending fibers (Oliver and Morest 1984), but they also contain local collaterals of intrinsic IC axons (Sect. 6.5.2). The presence of fibrodendritic laminae is the basis of the tonotopic organization found in the ICC (Fig. 6.2A, B).

6.2.2 Dorsal Cortex

In cats, the ICD is subdivided into two outer layers and two deeper layers (Morest and Oliver 1984). A difference between layers 3 and 4 is less clear in rodents (Fig. 6.1A), and the dorsal cortex is subdivided into three layers (Faye-Lund and Osen 1985). Layer 1 is the continuum of that in the ICL. The deepest layer forms the largest part of the ICD. The ICD receives more descending inputs and fewer lemniscal ascending inputs than the ICC (Coleman and Clerici 1987; Herbert et al. 1991). However, defining a distinct border between the ICC and ICD based on Golgi or fiber staining is challenging, if not impossible. Rather, it is more likely that there is a loose transition between these subdivisions.

Fig. 6.1 (continued) ICC than cortices except for *layer 2* of the ICL, which represents GABA modules. *Dashed lines* represent approximate boundaries for regions labeled in **A. (C)** Absence of VGLUT1 expression in the IC. Note that ventral to the ICC, mesencephalic trigeminal neurons express strong VGLUT1 mRNA. **(D)** Numerous IC neurons express VGLUT2. It is clear that neurons expressing VGLUT2 outnumber cells expressing VIAAT. (*Scale bar*: 1 mm for **A–D**) **(E)** Schematic diagram of the IC subdivisions in the rat and cat. The low frequency region in the ICC is contracted in rats while the size of the ventrolateral nucleus, *VLN*, (corresponding roughly to *layer 3* of ICL) is expanded in rats. [**A**–**D** modified from Ito et al. (2011) with permission of Wiley; **E** redrawn from Loftus et al. (2008) with permission of Elsevier]

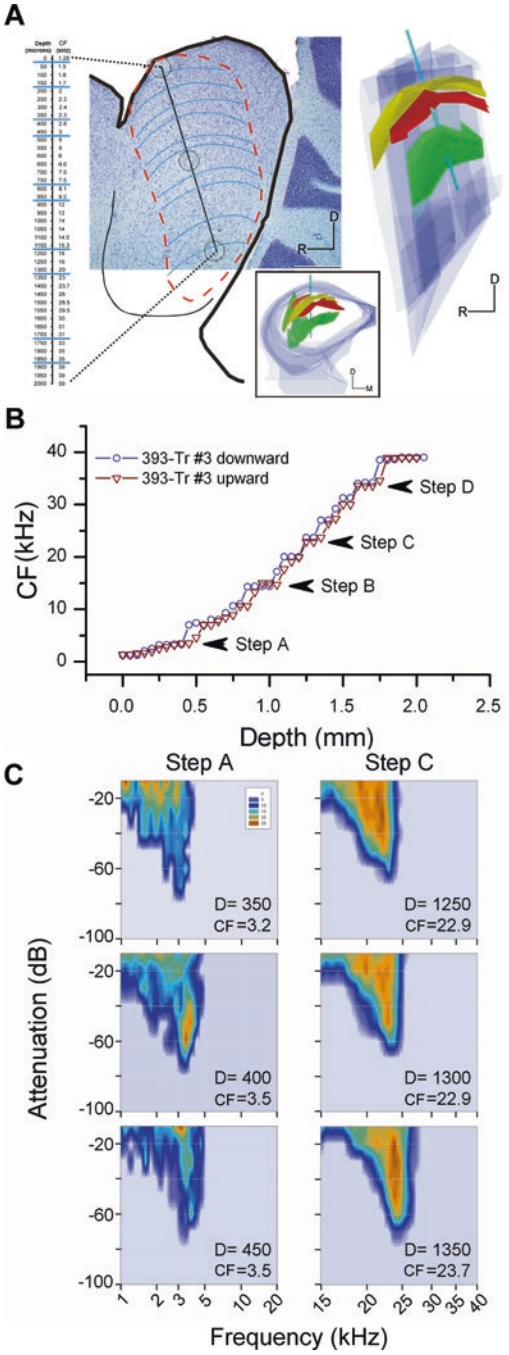

Fig. 6.2 Characteristic frequencies (CF) in the inferior colliculus. **(A)** ***Top left***: Sagittal section after Nissl staining; *dashed lines* show the boundaries of the fibrodendritic lamina in ICC. Frequency representation in the ICC along a 2000 μm electrode track (*black line*) identified

6.2.3 *Lateral Cortex*

The ICL is subdivided into three layers (Fig. 6.1). Since each layer has different types of inputs and outputs, they are likely to serve different functional roles. Ascending lemniscal inputs to the ICL, especially the peripheral layers, are scanty (Tokunaga et al. 1984). Instead, the auditory input originates mostly from the ICC. *Layer 1* is a thin, myelin-rich fibrous layer that is continuous with layer 1 of the dorsal cortex and brachium of the IC (Faye-Lund and Osen 1985; Oliver 2005). It contains numerous ascending fibers to the thalamus. *Layer 2* is composed of densely packed small neurons that form several clusters within a myelin-rich neuropil (Faye-Lund and Osen 1985). These two layers together constitute about one third of the maximum thickness of the ICL. *Layer 3* is larger than the other layers and may correspond to the ventrolateral nucleus of cats (VLN, Fig. 6.1E) (Faye-Lund and Osen 1985; Loftus et al. 2008). Layer 3 receives tonotopically organized axons that form band-like axonal plexuses almost orthogonal to the plexuses extending into the ICC (Saldaña and Merchán 1992; Malmierca et al. 1995).

6.2.4 *Rostral Cortex*

The ICR covers the rostral part of the IC. In coronal sections the ICR is easily recognized by the presence of many commissural fibers that interconnect both ICs and cross the ICR. The ICR may be homologous to a part of the intercollicular tegmentum described in the cat (Morest and Oliver 1984). Cytoarchitectonic features of the ICR or intercollicular tegmentum were revealed by Golgi preparations as very different from other IC regions (Morest and Oliver 1984). The neurons that populate this region are mostly multipolar cells of different sizes, with the largest ones being the most conspicuous (Malmierca et al. 2011). The function of the ICR is speculated to be multimodal integration (Oliver 2005).

Fig. 6.2 (continued) with three electrolytic lesions (indicated by *circles*); CF recorded at 50 μm intervals revealed frequency increases as a function of depth. Curves roughly perpendicular to the electrode track show the approximate orientations of the fibrodendritic laminae in ICC. CFs remain the same for roughly 150 μm and then change abruptly. ***Top right*:** Three-dimensional reconstruction of three axonal laminae. The recording electrode entered the ICC at a 10° angle with respect to the main dorsoventral axis of the ICC. Three different anatomical laminae formed by afferent axons are illustrated (*top*: 1.7 kHz lamina; *middle*: 1.8 kHz; *bottom*: 4.5 kHz). ***Bottom***: Frontal view of the same three-dimensional reconstruction after 90° rotation. (*D*, dorsal; *M*, medial; *R*, rostral) **(B)** A single electrode penetration downward (*circles*) and upward (*triangles*) along the same electrode track (*Tr*) through the ICC in which frequency response areas were obtained from multiunit clusters. (*CF*, characteristic frequency) **(C)** Frequency response areas from Step A and C shown in **B** recorded at 50 μm intervals; *Color scale* represents neuronal firing rate. *D*, Depth. [**A** anatomical data from Malmierca et al. (2005, 2008); **B** redrawn from Malmierca et al. (2008) with permission from the Society for Neuroscience; **C** redrawn from Oliver et al. (2011) with permission from Elsevier]

6.3 Neuron Types

There have been many attempts to classify neuron types in the IC. Classically, neurons in the IC were classified by dendritic morphology in Golgi impregnated material (Fig. 6.3). More recent studies utilize molecular profiles or electrophysiological properties to classify neuron types. These attempts have been only partially successful as the data indicate that there is no simple relationship between neuron classes defined with different methods. Most probably, a combination of several methods will be needed to draw a clearer portrait of IC neuron types.

6.3.1 Dendritic Morphologies of Neurons in the Inferior Colliculus

6.3.1.1 Dendritic Arborizations of Central Nucleus Neurons

Studies based on computer-assisted three-dimensional reconstructions of Golgi-impregnated material have shown that two main types of neurons populate the ICC (Fig. 6.3): disc-shaped or flat (F) neurons that have flattened dendritic arbors, and stellate cells or less flat (LF) neurons (Fig. 6.3B, C) with dendritic arbors that often extend across the laminae (Oliver and Morest 1984; Malmierca et al. 1993). The majority of ICC neurons (78%, cat; 67%, rat) are classified as disc-shaped or flat neurons.

The F and LF neurons differ in several respects, including dendritic arbor thickness, dendritic branching pattern, orientation, and location with regard to the laminae (Figs. 6.3, and 6.4B). In rats, the dendritic arbor of the F neurons lies parallel to a lamina that is about 50 μm wide. The laminae are separated by 100 μm-thick interlaminar compartments that are populated by the LF neurons. The dendritic arbor of these LF neurons is 100 μm wide and is less dense than the dendritic arbor of the F neurons (Malmierca et al. 1993). The dendritic arbors of most F and LF neurons are elongated and oriented in parallel with the ventrolaterally to dorsomedially oriented long axis of the laminae, although a few F neurons are oriented rostrocaudally (Fig. 6.4). A gradual shift takes place so that the orientation is more horizontal in the dorsolateral (low frequency) part of the nucleus and more vertical in the medial (high frequency) part (Malmierca et al. 1993).

6.3.1.2 Dendritic Morphologies of Cortex Neurons

Studies on the dendritic architecture in cortical regions of the IC are limited (Malmierca et al. 2011). Layer 1 of the ICD and ICL is made of small flattened neurons that are sparsely distributed (Faye-Lund and Osen 1985) and extend their dendrites parallel to the surface of the IC (Ito, unpublished observations). The deeper, slightly thicker layer 2 of the ICD consists of small and medium-sized, mostly multipolar neurons (Th+ cells in Fig. 6.7) (Ono et al. 2005). Layer 2 of the ICL also

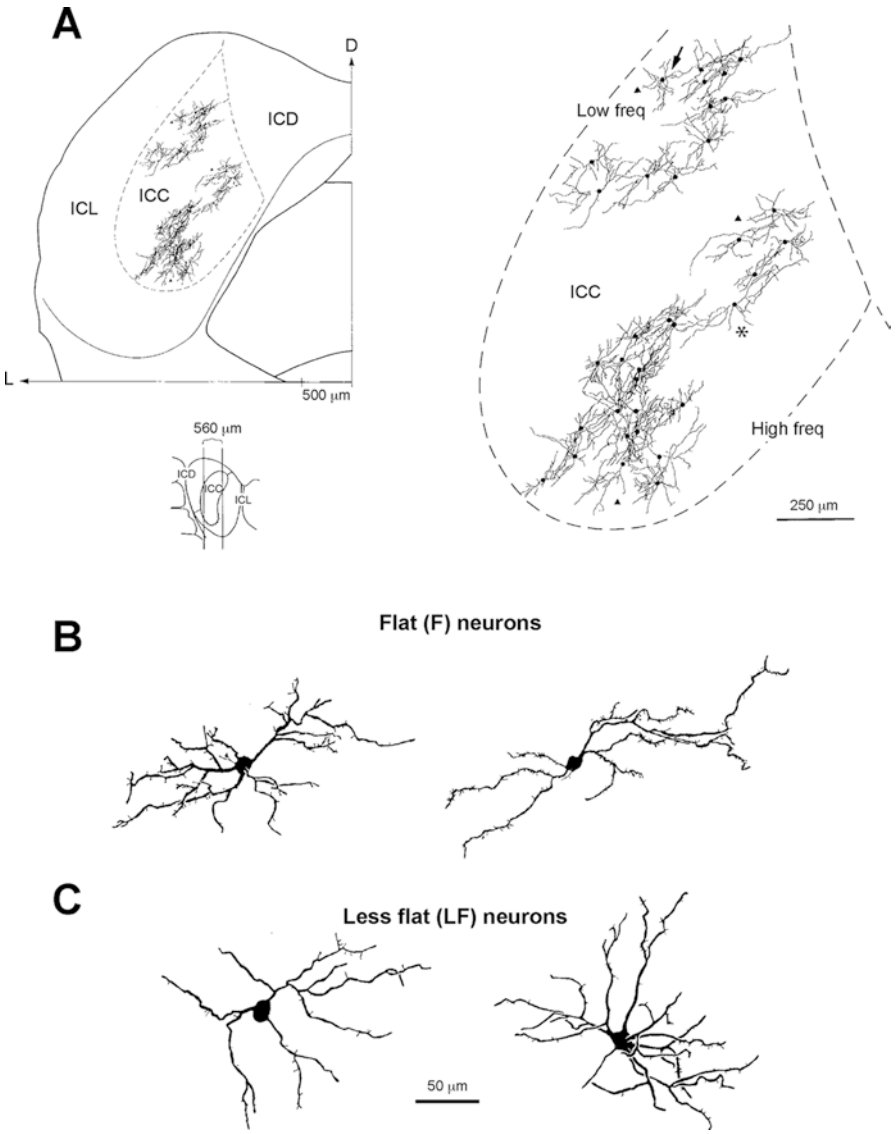

Fig. 6.3 Three-dimensional reconstructions of neurons within the central nucleus of the inferior colliculus from the low- and high-frequency regions, maintaining their anatomical relationships. **(A)** Illustration of the IC: central nucleus, *ICC*; dorsal cortex, *ICD*; lateral cortex, *ICL*. ICC shown enlarged on the right. *Inset* on left below panel indicates a sagittal section from where neurons were drawn. *Arrow* in the enlargement points to a perpendicular F neuron, *asterisk* is next to the longest cell, and *triangles* are adjacent to large cells in the outskirts of the ICC. **(B, C)** Camera lucida drawings of two flat neurons (*F*) and two less flat neurons (*LF*). (*Scale bars*: **A** enlargement 250 μm; **B, C** 50 μm) [Redrawn from Malmierca et al. (1993) with permission from Wiley]

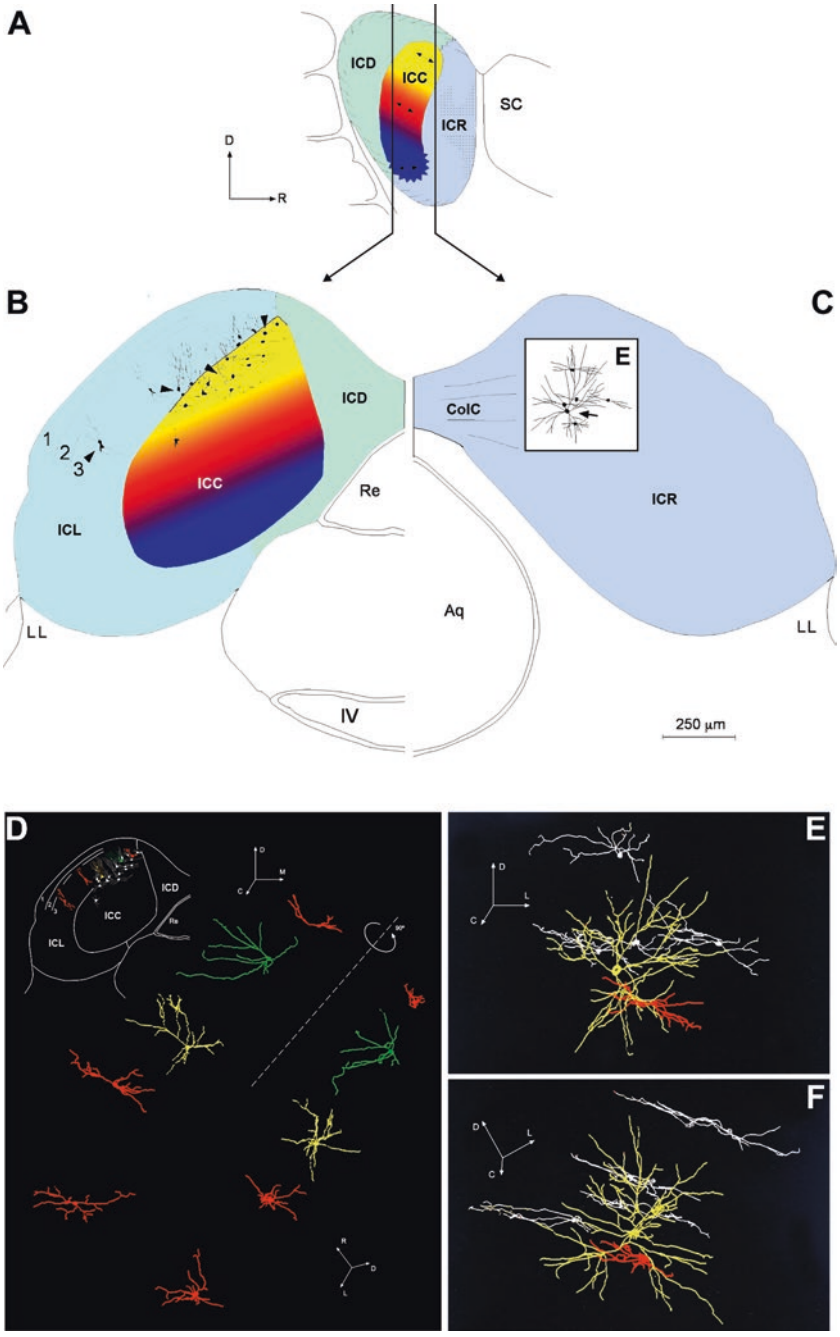

Fig. 6.4 Camera lucida drawings of a transverse section through the inferior colliculus (IC) of an adult rat. **(A)** Diagram illustrating the divisions of the IC. **(B)** Left IC is from a more caudal plane as indicated in the sagittal diagram in **A**. The left IC shows 7 flat neurons from the low frequency

contains small cells, but they form distinct clusters. Layer 3 of the ICD contains at least two types of neurons: large multipolar neurons and transitional neurons with elongated dendritic arbors that parallel the orientation of the ICC laminae and are located at the border between the ICC and the ICD (Malmierca et al. 2011).

Three-dimensional reconstructions of ICL neurons have shown that in addition to small and medium-sized cells, layer 3 contains large multipolar cells, especially ventromedially and rostrally, which makes the border with the ICC appear blurred (Fig. 6.1) (Loftus et al. 2008). In contrast, the dorsolateral portion has three morphologically distinct neuron types: bitufted, pyramidal-like, and chandelier. The dendritic orientations of these neurons mark a border with the ICC (Fig. 6.4B, D) (Faye-Lund and Osen 1985; Malmierca et al. 2011). Classical studies in the mouse by Willard and Ryugo (1983) described "large stellate cells with elongated dendritic arbors whose axes are oriented perpendicular to the pial surface." These types of neurons and distinct inputs to each layer suggest that the ICL possesses a cortical-like neuronal architecture, as originally described by Ramón y Cajal in 1902 (Malmierca et al. 2011).

Finally, neurons in the ICR lack a distinct dendritic orientation, so there is no indication of layering or anisotropy in the tissue (Malmierca et al. 2011). The neurons that populate this region are mostly multipolar cells of different sizes. The dendritic trees of large multipolar neurons are made of four or more thick dendritic processes that branch repeatedly without any preferred orientation and exhibit a few pedunculated spines. These neurons have the largest dendritic arbors in the entire IC (Fig. 6.4E, F).

6.3.2 Neurotransmitters in the Inferior Colliculus

Most IC neurons are considered to use GABA (gamma-aminobutyric acid) or glutamate as their neurotransmitter (see Fig. 6.1B–D). The use of glycine as a neurotransmitter is unlikely in the IC neurons since GLYT2 (necessary for the glycinergic

Fig. 6.4 (continued) region of the ICC and 16 neurons in the adjacent ICL. *Arrowheads* indicate some bitufted neurons. Some of the neurons are reconstructed in **D** (*scale bar* for B & C only). **(C)** The right IC showing neurons at the border zone between the rostral part of the ICC and the ICR with one typical large multipolar cell (*arrow*) and some flat neurons of the ICC. The same group of neurons is reconstructed in **E** and **F**. **(D)** Three-dimensional reconstruction of pyramidal (*yellow*), bitufted (*red*), and chandelier (*green*) neurons selected from the group of ICL neurons shown in the left IC in **B** and reproduced in the *inset at the upper-left* corner. The neurons are shown as drawn in the transverse section and then rotated about 90° until seen from a dorsolateral view with the neurons on end. Note that the cross section of the cells is cylindrical and not flattened. **(E, F)** Three-dimensional reconstructions of a selected group of neurons shown in **C** (right IC) from the transversely cut section at the border zone between the ICC and the ICR. The *yellow neuron* is a typical large multipolar neuron from the ICR while the *white neurons* are flat (*F*) neurons and the *red* is a less-flat (*LF*) neuron from the ICC (**E** as drawn in **B**; **F** after being rotated until seen on edge). The caudal part of the dendritic tree of the ICR neuron interdigitates with the F and LF neurons in this border zone. (*Aq*, aqueduct; *C*, caudal; *CoIC*, commissure; *D*, dorsal; *ICC*, central nucleus; *ICD*, dorsal IC; *ICL*, lateral IC; *ICR*, rostral IC; *LL*, lateral lemniscus; *SC*, superior colliculus; Re, recesus IV ventricle; *IV*, trochlear cranial nerve) [Redrawn from Malmierca et al. (2011) with permission from Elsevier]

phenotype) (Aubrey et al. 2007) is not expressed in the IC (Tanaka and Ezure 2004). The following sections include a description of IC neurons that use one of the two classical neurotransmitters and then a brief discussion of other neurotransmitters/neuromodulators follows.

6.3.2.1 Glutamate and GABA are Expressed in the Entire Inferior Colliculus

Numerous glutamatergic neurons are present in the IC. Electrical stimulation of the brachium of the IC elicited glutamate-receptor-mediated excitatory responses in medial geniculate neurons (Hu et al. 1994), suggesting that many IC ascending fibers are glutamatergic. Uptake of D-[^{3}H]aspartate by synaptic terminals of IC axons also suggested the presence of glutamatergic neurons in the IC (Saint Marie 1996). Indeed, numerous IC neurons express mRNA for vesicular glutamate transporter 2 (VGLUT2) (Fig. 6.1D) (Ito et al. 2011), which takes up cytoplasmic glutamate into synaptic vesicles (Fremeau et al. 2001). Messengers for the other isoforms of VGLUT (VGLUT1 and VGLUT3) are not expressed in adult IC (Fig. 6.1C) (Ito et al. 2009, 2011).

The presence of GABAergic neurons in the IC is well established, and they make up 20–30% of all IC neurons (Oliver et al. 1994; Merchán et al. 2005). The mean diameter of GABAergic neurons is larger than that of non-GABAergic neurons (Oliver et al. 1994; Merchán et al. 2005) and, indeed, the largest IC neurons are GABAergic (Oliver et al. 1994; Ito et al. 2009). IC GABAergic neurons show large diversity in size and are heterogeneously distributed (Fig. 6.1B). GABAergic neurons are more abundant and have higher density in the ICC than in the cortices (Merchán et al. 2005) except for the GABA modules in layer 2 of the ICL (Chernock et al. 2004), which are strongly positive for glutamic acid decarboxylase (GAD), a key enzyme in GABA synthesis. The GABAergic neurons in the GABA modules are likely to be a distinct neuron type (see Sect. 6.3.4). On the other hand, GABAergic neurons in the other part of the IC can be classified into at least 2 categories: large and small GABAergic (LG and SG) neurons (Fig. 6.5) (Ito et al. 2009; Ito and Oliver 2012). These two types receive different inputs and target different regions (Sect. 6.5.3). GABAergic neurons can be either disc-shaped or stellate (Ono et al. 2005); however, it seems that LG neurons are mostly stellate (Oliver et al. 1994; Ito and Oliver 2012). Most GABAergic neurons are likely to colocalize parvalbumin (Chernock et al. 2004).

6.3.2.2 Neuromodulators are Common in the Cortex

Several molecules that act as neuromodulators are expressed in the cortices of the IC. Nitric oxide, which is considered to be a retrograde messenger, is produced by ICD and ICL neurons (Coote and Rees 2008; Loftus et al. 2008). Enkephalin-expressing neurons are found in the ICD and in layers 1 and 3 of the ICL, with fewer in the ICC (Nakagawa et al. 1995). Since IC neurons express opioid receptors (Tongjaroenbuangam et al. 2006), the enkephalin may act locally. Layer 2 receives

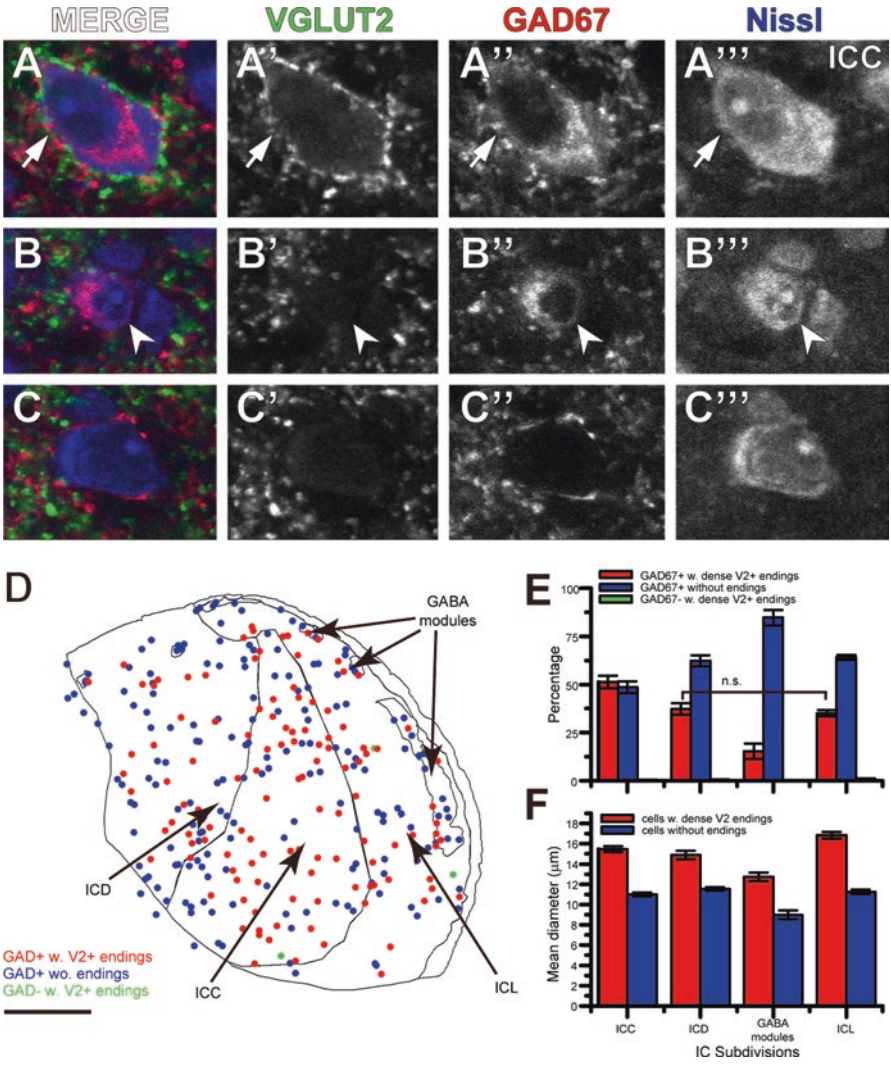

Fig. 6.5 Two classes of GABAergic neurons in the inferior colliculus (IC). **(A–C)** Confocal images of large GABAergic neurons (*arrows in A*), small GABAergic neurons (*arrowheads in B*), and nonGABAergic neurons (*C*) in the central nucleus (*ICC*). The large GABAergic (LG) neuron had a GAD67-positive (*3rd column*) large soma that was encircled by dense VGLUT2-positive (*2nd column*) terminals. The small GABAergic (SG) and GAD67-negative Nissl-stained (*4th column*) cell bodies lacked the dense VGLUT2-positive axosomatic terminals. **(D)** Distribution of GABAergic neurons. *Red dots* (GAD+ with V2 endings) indicate LG cell bodies; *blue dots* (GAD+ without endings) indicate SG cell bodies. *Green dots* are GAD67-negative cell bodies with dense VGLUT2-positive axosomatic terminals (GAD− with V2+ endings), which were rare. **(E)** Histogram illustrating relative percentage of the three neuron types shown in **D**; LG neurons were more commonly found in the ICC and were less common in the GABA modules (*scale bar:* 500 µm). **(F)** Histogram illustrating mean diameter of GABAergic somata: in all subdivisions, LG neurons had larger mean diameters than SG neurons. (*GABA*, gamma-aminobutyric acid; *GAD*, glutamic acid decarboxylase; *ICD*, dorsal IC; *ICL*, lateral IC; *VGLUT*, vesicular glutamate transporter) [Modified from Ito et al. (2009) with permission from the Society for Neuroscience]

strong cholinergic inputs (Henderson and Sherriff 1991). The neuropeptide Y-expressing neurons are mainly present in layer 2 of the ICL (Nakagawa et al. 1995). It appears that other neuropeptides, such as somatostatin, substance P, and cholecystokinin, are also expressed mainly in the ICD and ICL (Wynne et al. 1995; Wynne and Robertson 1997). These data suggest that many neuromodulators control layer-specific activity of the IC cortex. It should be noted, however, that some neuromodulators, like acetylcholine, serotonin, or noradrenaline, also innervate the ICC diffusely (Henderson and Sherriff 1991; Klepper and Herbert 1991; Schofield and Hurley, Chap. 9).

6.3.3 Physiological Classes of Neurons in the Inferior Colliculus

There is a large diversity of auditory-evoked responses in the IC. Some of the responses are inherited from neurons in lower brain stem nuclei, but others emerge de novo from the integration of multiple inputs originating in diverse nuclei. It should be emphasized that the intrinsic membrane properties of IC neurons also play a role in encoding sound-evoked discharges.

6.3.3.1 Intrinsic Physiological Properties

IC neurons exhibit a variety of intrinsic membrane properties that can modulate inherited sound-evoked activity. Proportions of neuron types are different between subdivisions and may explain the differences in sound-evoked activity across IC subdivisions, at least in part.

Six Firing Patterns in the Central Nucleus

In vitro studies using brain slice preparations have demonstrated that ICC neurons show one of six firing patterns in response to depolarizing current injection (Fig. 6.6) (Sivaramakrishnan and Oliver 2001). Onset neurons (8.6% of ICC neurons; Fig. 6.6B) can be quickly repolarized after both single and summed depolarizing currents so that they are well-suited for temporal coding (Peruzzi et al. 2000) but cannot encode the duration or intensity of sounds (Sivaramakrishnan and Oliver 2001). Sustained neurons exhibit a heterogeneous array of responses that can be grouped into five types: (1) sustained regular (19.2% of ICC neurons; Fig. 6.6A); (2) pause/build (12.5%; Fig. 6.6C); (3) rebound regular (10.6%; Fig. 6.6D); (4) rebound adapting (25%; Fig. 6.6E); and (5) rebound transient (21.1%; Fig. 6.6F) (Sivaramakrishnan and Oliver 2001). Sustained-regular, pause/build, and rebound-regular neurons show sustained firing with constant

interspike intervals throughout injection of depolarizing current (Fig. 6.6). Since they have a linear voltage response to a wide range of input currents, they may have linear rate-level functions to sound. The relatively simple properties of onset neurons and sustained-regular neurons imply that these neuron types may serve to relay intensity and temporal information. On the other hand, the remaining neuron types, which make up about 70% of ICC neurons, substantially modify inputs and create de novo responses.

Pause/build neurons have an A-current. Hyperpolarization that precedes depolarization, such as that produced by a previous after-hyperpolarization or an inhibitory postsynaptic potential (IPSP), removes inactivation of the A-current and modifies the initial part of the neural response. This produces a buildup response or a pause in firing after an onset spike. The pause duration is proportional to the magnitude of hyperpolarization. Therefore, the pause/build cells may show temporal interaction between two stimuli with a time lag smaller than 100 ms.

Rebound neurons fire just after the cessation of hyperpolarization and may code offset of inhibition. Each of the three types of rebound neurons show different degrees of adaptation of firing to depolarization. Reboundregular neurons do not exhibit adaptation, whereas reboundtransient neurons show only phasic activity. Reboundadaptation neurons start to show adaptation for stimuli longer than 200 ms.

Tan et al. (2007) demonstrated firing properties of rodent IC neurons to current injections in vivo. In living animals, spontaneous excitatory postsynaptic potentials (EPSP) are common and affect firing regularity. Although responses to depolarizing current were generally similar to the slice studies, there were several differences. These authors found accelerated firing in 11% of cells, but they did not observe onset neurons that fired only a single spike. Burst-firing neurons were seen more commonly (15%) in the in vivo preparations than in vitro.

Firing Patterns in the Cortex

In contrast to the six firing patterns of ICC neurons described in Sect. 6.3.3.1.1, the IC cortex appears to be composed of fewer neuron types. In the ICL, the majority of neurons studied (66%) showed regular firing, and transient neurons were never observed (Ahuja and Wu 2007). ICL neurons have a lower threshold of firing than ICC and ICD neurons (Li et al. 1998). The relatively uniform membrane properties and the low thresholds of ICL neurons imply that the ICL may relay auditory information from the ICC (Ahuja and Wu 2007).

In the ICD, almost all neurons studied (91%) showed sustained firing; the rest showed a buildup response (Sun and Wu 2008). Half of the sustained neurons exhibited a rebound response after hyperpolarizing current injection. Interestingly, preceding hyperpolarization modifies the response to depolarization in more than half of the non-rebound neurons. These findings suggest that most ICD neurons modify their firing activity based on preceding inhibition.

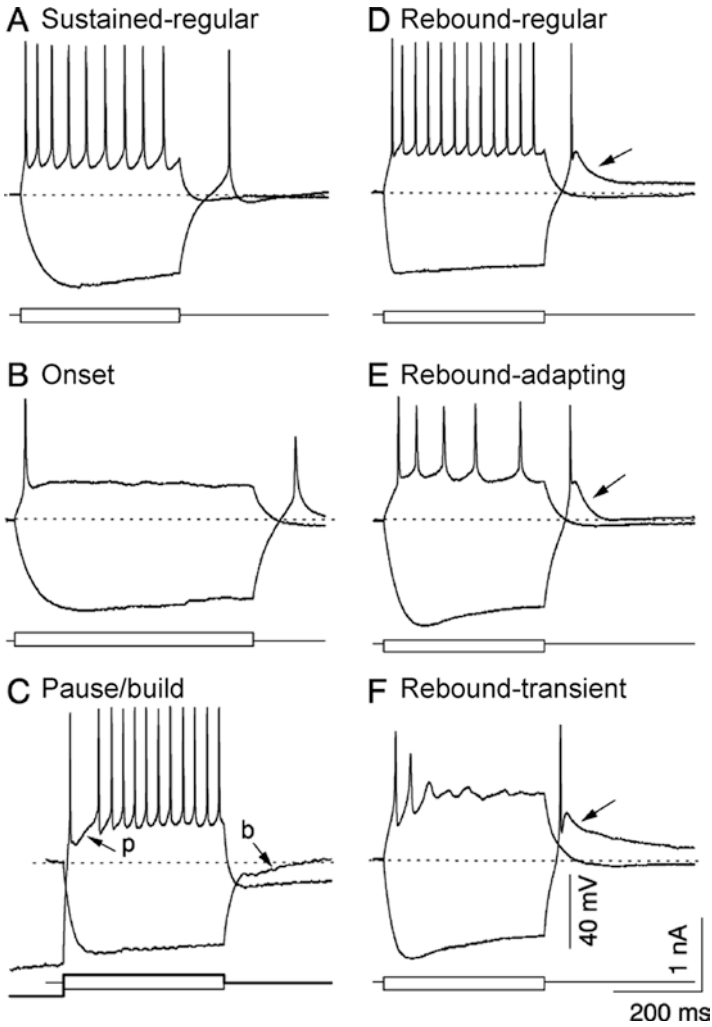

Fig. 6.6 The six firing patterns found in the inferior colliculus after injection of depolarizing and hyperpolarizing current pulses. In each panel, the *top two traces* are the voltage response to each current pulse (*bottom traces*). **(A)** Sustained-regular and **(B)** onset firing to depolarization with an anode-break spike and no calcium rebound following hyperpolarization. **(C)** Pause/build response to depolarization after prehyperpolarization and no anode-break spike after hyperopolarization. This cell shows a pause in firing (*p*) after the first spike; the response to a hyperpolarizing current shows a buildup response (*b*). **(D)** Sustained regular firing to depolarization with an anode-break sodium spike and a calcium rebound following the hyperpolarization. **(E)** Sustained firing with adaptation and calcium-sodium rebound activity. **(F)** Transient response to depolarization with calcium-sodium rebound activity. [Figure kindly provided by Dr. Douglas L. Oliver; redrawn from Sivaramakrishnan and Oliver (2001) with permission from the Society for Neuroscience]

6.3.3.2 Responses to Sound

Tuning of Cortex Neurons

A fundamental physiological feature of the ICC is its tonotopic organization. Neurons located in dorsolateral laminae respond to low frequency sounds, and neurons located more ventrally respond to progressively higher frequency sounds. However, this representation does not appear to reflect a continuous mapping—fine grained tonotopic mapping studies have demonstrated a distinct stepwise organization in the progression of characteristic frequencies (CF) (Schreiner and Langner 1997; Malmierca et al. 2008). Moreover, independent data from single neurons showed that CFs at octave intervals of approximately one-third are more prevalent than others (Malmierca et al. 2008). Thus, a narrow range of CFs is represented within each isofrequency lamina (Fig. 6.2B, C). Since the physiological step width is similar to the laminar thickness, and the frequency increase is comparable to one critical band width, the isofrequency laminae have been postulated to correlate with critical bands (Schreiner and Langner 1997).

An elegant study recently explored the possible relationships between the microstructure of the cochlear map and the tiered tonotopy observed in the IC (Shera 2015). The stepwise tonotopy may be an emergent property arising from wave reflection and interference within the cochlea, a mechanism similar to that responsible for the microstructure of the hearing threshold (Shera 2015). Each lamina of the ICC also shows a highly organized representation of both spectral and temporal features of the acoustic signal. An axis that maps the best modulation frequency appears to be oriented orthogonal to the frequency or tonotopic axis and within the plane of the laminae (reviewed by Schreiner and Langner 1988, 1997).

Single-unit recording studies of ICC neurons in response to pure tone stimulation have revealed that IC neurons show a large variety of frequency response areas that include both V-shaped (Fig. 6.2C) and non-V-shaped ones (Palmer et al. 2013). The non-V-shaped response types form a heterogeneous group that includes closed, narrow, low- and high-tilt, and multipeaked response areas. In addition, ICC neuron responses produce different types of peristimulus time histograms including onset, on-sustained, pauser, sustained, and regular responses (Duque et al. 2012). The ICC neurons are also sensitive to the duration of the sound stimuli (Pérez-González et al. 2006) and to binaural stimulation. Thus ICC binaural responses can be suppressive, summative, or mixed (Zhang and Kelly 2010). Binaural suppression responses are more numerous at high frequencies and summation is more common at low frequencies. These characteristics of binaural interaction likely reflect the time course of converging excitatory and inhibitory synaptic inputs to ICC neurons as well as the intrinsic membrane properties of those neurons. Studies based on the iontophoretic application of GABA and glycine antagonists have shown that neural inhibition contributes to the binaural responses of neurons in the IC (Faingold et al. 1989, 1991). The ICC neurons show responses to amplitude modulation and frequency modulation (FM) as a function of the modulation frequency and other parameters (Moller and Rees 1986; Rees and Moller 1987).

Novelty Detection in Cortex Neurons

Studies on the neuronal responses of cortical regions of the IC are still sparse, but there is evidence that these neurons exhibit multisensory integration that mirrors a similar integration at higher levels of the nonlemniscal auditory pathway (reviewed by Malmierca and Ryugo 2011). Another prominent feature of neurons in the nonlemniscal IC regions is the phenomenon of stimulus-specific adaptation (SSA). This property is a specific adaptation of neuronal responses to a repeated stimulus that does not fully generalize to other stimuli. It provides a mechanism for emphasizing rare and potentially interesting sensory events. The SSA phenomenon has been linked to deviance detection, auditory memory, recognition of acoustic objects, auditory scene analysis, and behavioral habituation (Netser et al. 2011; Ayala and Malmierca 2012). Moreover, SSA may be a component of short-term memory in neuronal networks since it creates a nontrivial dependence of neuronal responses on the history of the stimulation. A series of recent studies of cortical IC neurons (i.e., nonlemniscal neurons of the IC) demonstrated that the great majority exhibit SSA, display transient onset responses, and have broad frequency response areas (Pérez-González et al. 2005, 2012). As described in Sect. 6.3.1.2, neurons in the ICD and ICR regions possess widespread dendritic arbors (Malmierca et al. 2011) and broader frequency tuning than those in the ICC (Duque et al. 2012). Although SSA was originally described in the cat primary auditory cortex and was suggested to be an emergent property of the auditory cortex (AC) (Ulanovsky et al. 2003), IC neurons do not inherit their SSA sensitivity from the AC (Anderson and Malmierca 2013). However, they may be strongly modulated in a gain control fashion (Anderson and Malmierca 2013) directly through the corticofugal projections (Ayala et al. 2015) or indirectly via cholinergic inputs (Ayala and Malmierca 2015).

6.3.4 Dendritic Morphologies, Neurotransmitters, and Physiological Properties

As the numbers of morphological and physiological classes are both relatively small, one might expect a simple one-to-one relationship between dendritic morphology and firing properties. However, the dichotomy of dendritic morphology (disc-shaped or stellate) does not generally predict differences in physiological properties. Both disc-shaped and stellate cells appear to be subdivided into several physiological classes.

Correlations between intrinsic membrane properties and dendritic arborization was addressed in slice studies (Reetz and Ehret 1999; Peruzzi et al. 2000). Although both transient and sustained responses were observed, the ratio of each response differed across studies. Interestingly, the ratio of neuron types based on dendritic arborization also differed among the studies, and it is likely that the higher the percentage of neurons with unoriented dendrites, the higher the percentage of onset responses. Indeed, an in vivo juxtacellular study demonstrated that the onset

response was characteristic of stellate neurons but not of those with oriented dendrites (Wallace et al. 2012). Further, rebound neurons may have larger somata with more complex dendritic trees, whereas buildup neurons have smaller somata with a simpler dendritic tree (Peruzzi et al. 2000).

Ono et al. (2005) studied GABAergic neurons in the IC by using GAD67-GFP mice in which GABAergic neurons express GFP (green fluorescent protein). They demonstrated that GABAergic neurons can be subdivided into several classes by their dendritic arborizations and intrinsic membrane properties (Fig. 6.7).

A common feature of GABAergic neurons is the presence of a depolarizing sag, which may enhance temporal precision in response to synaptic inputs. The GABA neurons in layer 2 of the ICL (Th+ in Fig. 6.7), in other words, the GABA modules, form a single distinct class of IC neurons since they share a small, oriented dendritic morphology and a transient response with a hump in response to current injections, which is only expressed in these neurons. Regular-sustained neurons (RS in Fig. 6.7)

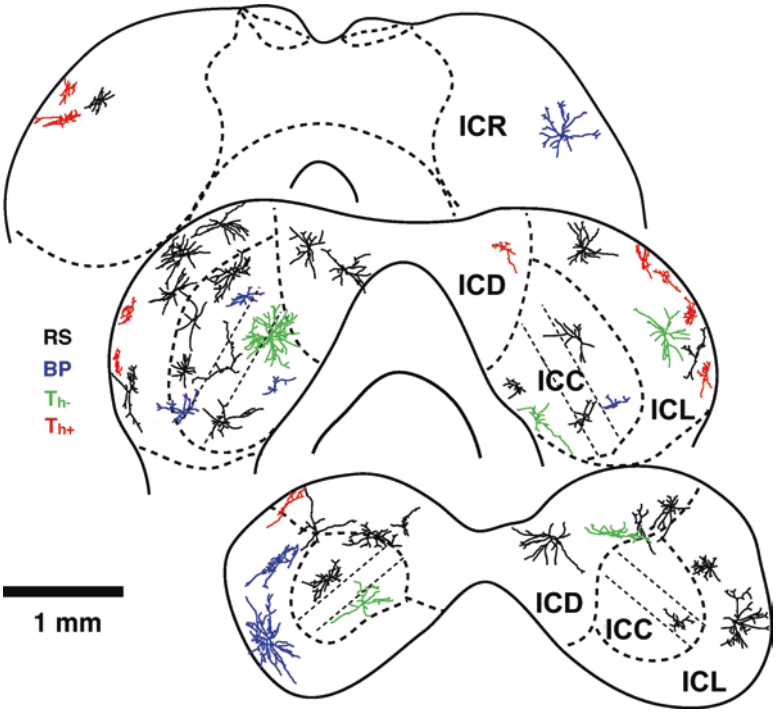

Fig. 6.7 Dendritic arborization and distribution of GABAergic neurons in the inferior colliculus (IC) for which intrinsic properties were identified and classified into regular-sustained (*RS*, *black*), buildup-pauser (*BP*, *blue*), transient with hump (*Th−*, *green*), or transient without hump (*Th+*, *red*). *Thick dashed lines* indicate the border of IC subdivisions, and *thin dashed lines* indicate laminae in the central nucleus. (*ICC*, central nucleus of IC; *ICD*, dorsal nucleus of IC; *ICL*, lateral nucleus of the IC; *ICR*, rostral nucleus of the IC) [Figure kindly provided by Dr. Munenori Ono; modified from Ono et al. (2005) with permission from Elsevier]

are commonly found in every subdivision. Buildup-pauser neurons (BP in Fig. 6.7) are likewise common in ICC and ICL but almost absent in the ICD. These two neuron types do not correlate with specific dendritic morphologies. A minority of GABAergic neurons in the ICC and ICD express a transient response without a hump (Th− in Fig. 6.7) and are large stellate neurons. Some of these GABAergic neurons may correspond to those classified as LG neurons that are contacted by dense excitatory axosomatic synapses and project to the thalamus (Ito et al. 2009; Ito and Oliver 2012). Geis and Borst (2013) demonstrated that LG cells in mouse ICD show an EPSP with a short delay at the onset of sound, have low input resistance, and exhibit a depolarizing sag in response to hyperpolarizing current. These characteristics imply that activation of the LG cells requires the occurrence of many EPSPs within a short period of time (Ito and Oliver 2014). Geis and Borst (2013) also noted that adaption to depolarization current is more commonly seen in neurons with larger cell bodies.

Since stellate neurons extend dendrites into neighboring isofrequency laminae, they may be associated with spectral integration. In an intracellular study, Kuwada et al. (1997) reported that three neurons that exhibited sideband IPSPs had stellate morphology. Likewise, in slice preparations stellate cells showed both EPSPs and IPSPs in response to electrical shocks in the lateral lemniscus, but neurons with oriented dendrites showed EPSPs alone, suggesting the presence of sideband inhibition in the stellate cells (Reetz and Ehret 1999). Some IC neurons respond strongly to FM sweeps. It is very likely that these neurons integrate both spectral and temporal information. They are large neurons (Kuo and Wu 2012), and some of them also had unoriented dendrites (Poon et al. 1992).

6.4 Extrinsic Inputs to the Inferior Colliculus

6.4.1 Ascending Inputs

Since the main goal here is to highlight the different patterns of ascending inputs between ICC and IC cortical regions, the reader is referred to Cant and Oliver (Chap. 2) for further details on the organization of the auditory ascending pathways. Lemniscal ascending fibers from the cochlear nuclei (CN), superior olivary complex (SOC), and the nuclei of the lateral lemniscus (NLL) mainly target the ICC, and they are tonotopically organized. Bands of axons and terminals are labeled in the ICC after small injections of anterograde tracers into the CN, SOC, or NLL (reviewed by Oliver and Huerta 1992; Malmierca 2015).

A portion of the IC cortex, mainly the deeper layers, also receives tonotopically organized afferent inputs (details in Oliver and Huerta 1992). Band-like ascending lemniscal fibers arising from the CN and NLL invade the deep layers of the ICD. In the cat, ventral CN (VCN) axons are found in layers 3 and 4, while dorsal CN (DCN) axons are restricted to layer 4, which is adjacent to the ICC. Layer 3 of the ICL also receives inputs from the same nuclei as the deeper layers of the

ICD. Ventral NLL (VNLL) axons appear to send fewer projections into the collicular cortices than dorsal or intermediate NLL (DNLL or INLL) axons (Whitley and Henkel 1984).

In contrast to ICC, the IC cortex receives inputs from various nonauditory subcortical nuclei (reviewed by Gruters and Groh 2012). Laminar organization of the IC cortex reflects different combinations of nonauditory input sources. Layer 1 of the ICD and ICL receives visual inputs from the contralateral retina (Itaya and Van Hoesen 1982). Layer 2 receives dense fibers from the dorsal column nuclei (Wiberg et al. 1987). Terminals of these axons form several patches that seem to correspond to the GABA modules (Lesicko and Llano 2015). Therefore, neurons in GABA modules may receive somatosensory information and transfer onset inhibition to other neurons. All layers receive nondopaminergic inputs from substantia nigra pars lateralis (Yasui et al. 1991). Neurons in the globus pallidus appear to project to upper layers of the ICD and ICL (Shammah-Lagnado et al. 1996). Cholinergic fibers that originate from midbrain tegmental nuclei (Motts and Schofield 2009) terminate densely in layer 2 and sparsely in other layers (Henderson and Sherriff 1991). Noradrenergic fibers that arise from locus coeruleus are dense in layers 2 and 3 while serotonergic fibers from the dorsal raphe nucleus are dense in layer 1 (Klepper and Herbert 1991). Considering the dendritic orientation and morphology of neurons in the deeper layers of the IC cortex, these neurons are likely to integrate visual (layer 1), somatosensory (layer 2), and auditory (layer 3) information as well as behavioral context via the substantia nigra and globus pallidus. The layer preference of monoaminergic and cholinergic innervation suggests that the modes of multimodal integration in the IC cortex can be altered by behavioral and mental states.

6.4.2 Descending Inputs

The descending pathways from the AC are described by Cant and Oliver (Chap. 2). Therefore, only the major differences in the patterns of descending inputs between ICC and IC cortex are summarized here. Glutamatergic pyramidal neurons located mainly in layer V but also a small number in layer VI (Games and Winer 1988) project to both ICs, although the ipsilateral projection is heavier than the contralateral one (Herbert et al. 1991; Saldaña et al. 1996). The ICC receives tonotopically organized fibers from the primary auditory cortex (A1) (Saldaña et al. 1996): the caudal low-frequency regions of A1 project to the dorsal laminae, and the rostral high-frequency regions project to the ventral laminae in the ICC (Saldaña et al. 1996).

The IC cortex receives inputs from multiple areas of the forebrain. The A1 neurons form tonotopically organized terminal areas in the ICD and ICL. The caudal low-frequency regions of A1 project to the dorsolateral laminae in the ICL and dorsal laminae in the ICD, which is the continuum of those in the ICC. The rostral high-frequency region projects to the ventrolateral laminae in the ICL and ventral laminae in the ICD (Saldaña et al. 1996). Secondary, multimodal auditory cortical

areas also project to the IC cortex. Area Te2 projects to layer 1, whereas Area Te3 projects to layers 2 and 3 of the ICD and ICL (Herbert et al. 1991). It is interesting to note that Areas Te2 and Te3 seem to correspond to the cat's posterior auditory field and the suprarhinal auditory field, respectively (Malmierca 2015), which constitute high-order cortical fields linked to the nonlemniscal auditory pathway.

Although the corticollicular projection is purely excitatory, electrical stimulation of the AC in cat (Mitani et al. 1983) or its inactivation in rat, using either tetrodotoxin (Nwabueze-Ogbo et al. 2002) or a cooling technique (Anderson and Malmierca 2013), produce not only excitatory but also inhibitory responses in IC neurons. Those studies indicate that the AC modulates IC responses through the activation of local inhibitory connections.

6.5 Microcircuits

Knowing the details of organization of the IC microcircuits is essential for gaining a better understanding of how auditory information is encoded in the IC. Thus far, most studies of IC microcircuitry have been restricted to the ICC and very little is known about the microcircuitry of the cortical areas.

6.5.1 Synaptic Domain Hypothesis

As described in Sect. 6.3.1.1, the ICC is composed of 150–200 μm sheets that form isofrequency laminae and interlaminar components. Neurons in one lamina share similar CFs within a range of about 0.3 octaves (Schreiner and Langner 1997; Malmierca et al. 2008). Other characteristics of sound are represented in a nonuniform fashion, although adjacent neurons tend to have similar responsiveness to sound (Chen et al. 2012). In an in vitro study in laminar slices, repetitive shocks to the lateral lemniscus revealed several zones showing different activities (Chandrasekaran et al. 2013). These observations are consistent with the concept that the laminae contain distinct functional zones. These functional zones are referred to as synaptic domains because they are created by specific shared inputs, at least in part (Casseday et al. 2002; Oliver 2005). Neurons in the same synaptic domain may share the same terminal field in the medial geniculate body (MGB), which is described later in this section (Cant and Benson 2007).

Earlier anterogradetracing studies had already revealed that projections from lower brainstem nuclei produce segregated terminal fields in the ICC but with various degrees of overlap (details in Oliver and Huerta 1992). These terminal zones have been examined in detail in the projections from CN and SOC. The projections from the two sides of the lateral superior olive (LSO) interdigitate, forming bands suggestive of a sublaminar organization within the isofrequency laminae (Shneiderman and Henkel 1987). Terminal fields of axons from DCN and LSO on

the same side overlap in the lateral part of the contralateral ICC, but the inputs from the DCN extend more medially than do those from the LSO (Oliver et al. 1997).

In more recent studies, focal injections of anterograde tracers were made in functionally defined zones of the medial superior olive (MSO) and LSO to reveal the organization of inputs to specific synaptic domains (Oliver et al. 2003; Loftus et al. 2004). Axons from two different regions of MSO with similar CFs but presumably different interaural time difference (ITD) sensitivities gave rise to overlapping terminal fields within a lamina, suggesting convergence of ITD information in the ICC (Oliver et al. 2003). Within the laminae representing low frequencies, axons from ipsilateral MSO terminate in the centraltocaudal part of the ICC, while those from the contralateral LSO terminate in the rostral ICC. Therefore, the main excitatory drives from the SOC appear to be largely segregated. On the other hand, axons from the ipsilateral LSO, which are mainly inhibitory, target the same domain as the ipsilateral MSO (Loftus et al. 2004). Since the MSO showed maximal discharge rates at the best ITD (peak-type responses) and the LSO showed minimal responses at best ITD (trough-type responses) (Joris and Yin 1995), the results suggested that ITD coding is different in the sublaminar domains.

Segregation of the terminal fields of ascending axons from different origins suggests that different synaptic domains receive unique combinations of inputs. By making medium-sized tracer deposits, Cant and Benson (2006) demonstrated patterns of ascending inputs to 74 injection sites that covered most parts of the gerbil IC. Three combinations of ascending inputs were identified: group 1 received substantial inputs from the MSO and LSO (>5% of total labeled cells), group 2 almost lacked inputs from these nuclei, and group 3 had few ascending inputs. Moreover, and importantly, the group categorization was a good predictor of the injection site: group 1 sites fell into the rostrolateral zone of the ICC while group 2 sites fell into the caudal ventromedial zone. Sites of both groups received substantial inputs from the CN, VNLL, and superior paraolivary nucleus of the SOC. Group 3 sites corresponded to the ICL and ICD. Group 1 might be further subdivided into dorsal and ventral parts with the dorsal part receiving more input from the MSO than the ventral part, which is dominated by inputs from the LSO. Once again, these data are consistent with the hypothesis that the IC is made of synaptic domains that receive unique combinations of inputs.

The unique combinations of inputs into each synaptic domain may create domain-specific responses to features of sound. By making small injections of retrograde tracers into physiologically characterized sites, Loftus et al. (2010) correlated anatomical and physiological features of synaptic domains of cat ICC. Based on the proportions of each input, three types of domains were classified. The first type (confined mainly to the caudal ICC) was characterized by inputs from the contralateral CN and ipsilateral VNLL, and physiologically the neurons exhibited monaural responses. The second type (confined to the dorsal ICC) was characterized by inputs from the MSO and ipsilateral LSO, and the neurons showed ITD sensitivity to low frequencies. The third type of domain (confined to the rostral ICC) was relatively heterogeneous but had in common inputs that arose bilaterally from the SOC nuclei, and the neurons showed ITD sensitivity to complex sounds.

Each synaptic domain has a characteristic ascending projection. Binaural and monaural domains in the gerbil ICC appear to target different regions in the ventral division of the MGB (the MGV) with some overlap (Cant and Benson 2007). The lateral zone of the ICC, which receives substantial inputs from the MSO and LSO, targets the rostral part of the MGV. In contrast, the medial zone, which lacks inputs from the MSO and LSO, targets the caudal part of the MGV. Overlap of inputs from the two zones is obvious in the ventral part of the MGV. These findings suggest the existence of parallel pathways from midbrain to thalamus such that each functional domain created in the IC projects in parallel to a functional domain of the medial geniculate.

6.5.2 Contributions of the Local Circuitry

The studies discussed in Sect. 6.5.1 emphasized the organization of ascending inputs within a synaptic domain. However, it was not possible to analyze the contributions of local axon collaterals in those tracer injection studies. Within the IC, a massive system of local collaterals provides a substrate for interactions among neurons (Fig. 6.8). The axonal arborization patterns of single neurons give the most detailed information about local circuitry, although the number of studies is limited due to the difficulty of filling individual IC neurons. Oliver et al. (1991) filled eighteen cat IC neurons with HRP and demonstrated that nearly all labeled neurons (except for one in the VLN) had local collaterals. Two ICC neurons with rostrocaudally oriented dendritic fields (disc-shaped cells) gave rise to axonal terminations confined to the fibrodendritic laminae.

Neurons that have dendrites with mediolateral orientation or no orientation (stellate cells) gave rise to axons with no orientation (Fig. 6.8A). Some cells had both a thick branch entering the brachium of the IC (an ascending projection branch; arrowheads in Fig. 6.8) and local collaterals. Wallace et al. (2012) examined eleven juxtacellularly labeled guinea pig ICC cells that had oriented dendrites and formed terminations within fibrodendritic laminae (Fig. 6.8B). The axonal plexuses of neurons with the CF higher than 1 kHz had a laminar thickness of about 200 μm, while those with lower CFs were less extensive. In concert with the extensive axonal plexuses in the low CF area (dorsal ICC), the volume of the dendritic arbor is reduced in the dorsal ICC neurons of mice (Reetz and Ehret 1999), suggesting that dorsal, low CF neurons form a less complex local circuitry than do ventral, high CF neurons.

Ito and Oliver (2014) used a viral tracer to investigate local and projection axons (e.g., Ito et al. 2007; Matsuda et al. 2009) and reconstructed axons of three glutamatergic neurons in the ICC and ICL. All of them had a laminar axon (Fig. 6.8C). One ICC cell formed two axonal plexuses extending from the ICC to ICD and had one plexus in the ICL. Although the virus has been shown to label very long projection axons (e.g., sympathetic preganglionic neurons; Ito et al. 2007) or highly arborized terminal bushes (e.g., nigrostriatal fibers; Matsuda et al. 2009), labeled axons outside the IC were not found in these three infected neurons, suggesting that they were

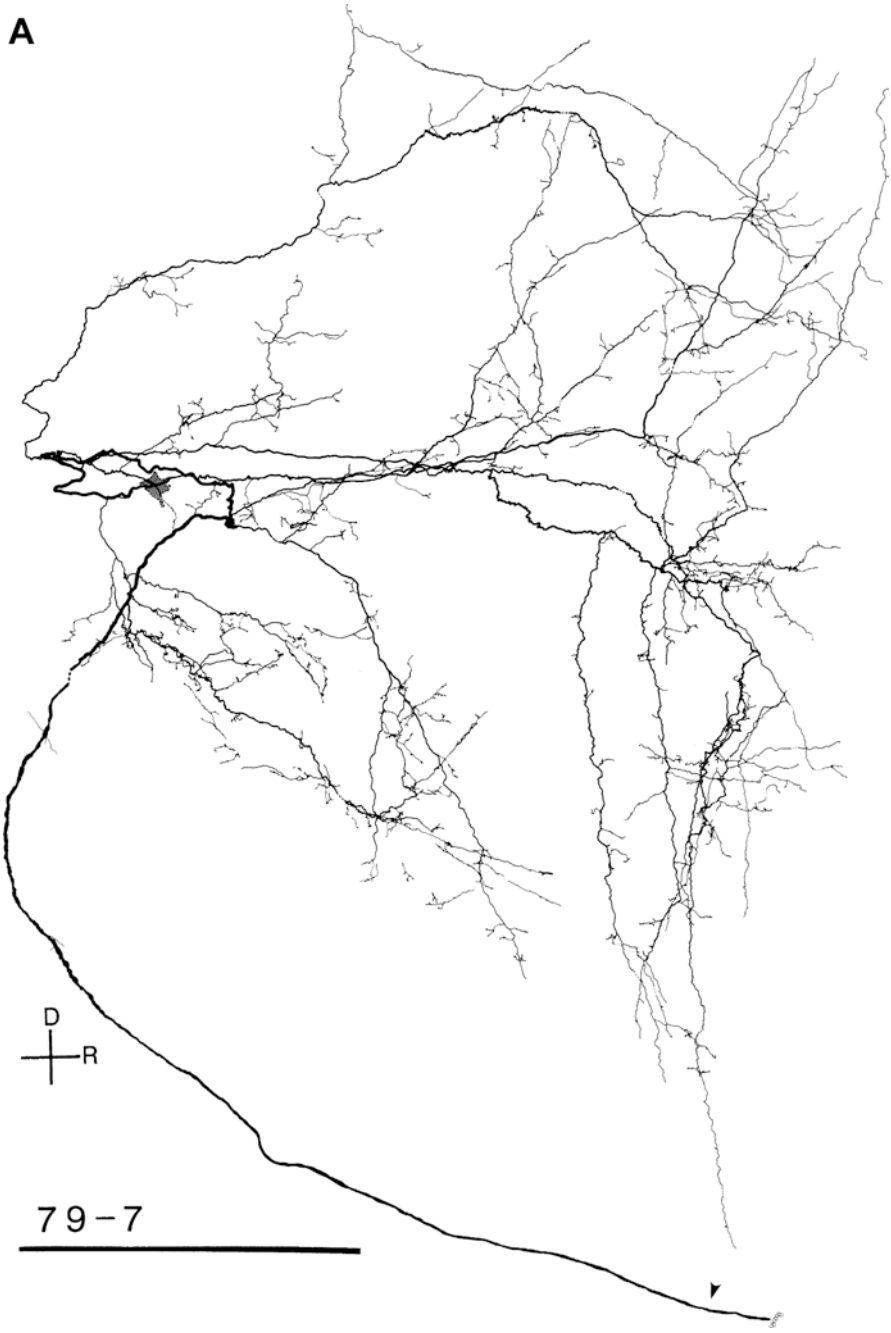

Fig. 6.8 (continued)

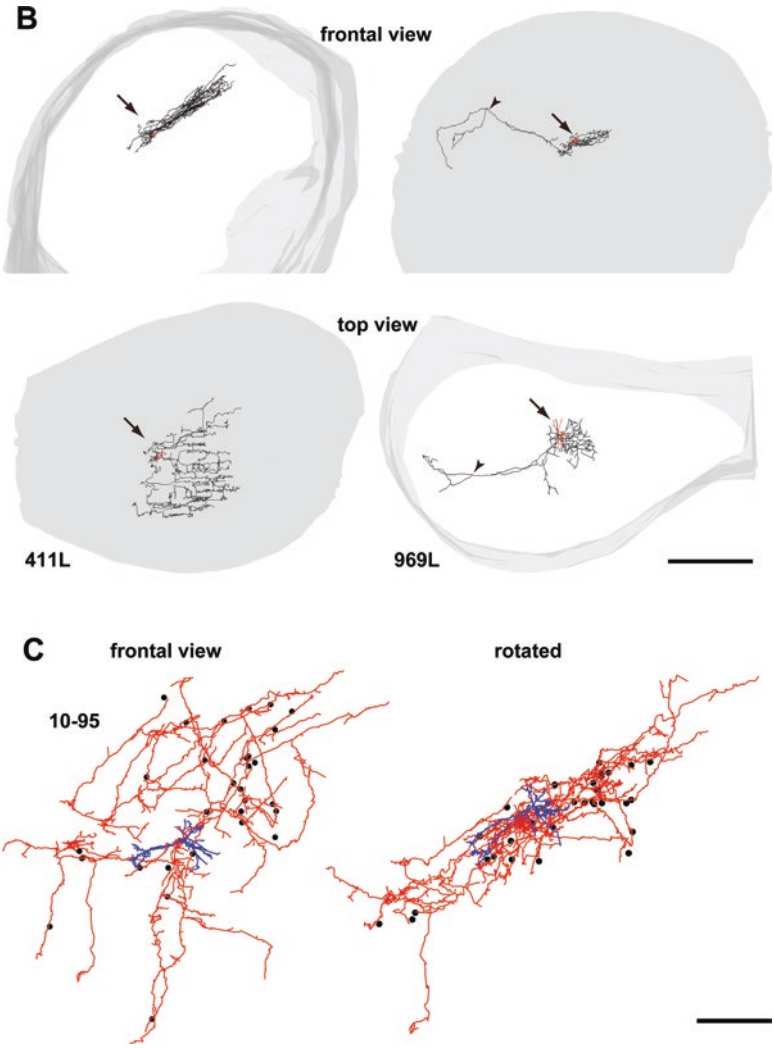

Fig. 6.8 Local axon collaterals of neurons in the inferior colliculus. **(A)** The axon of a mediolaterally oriented (presumably stellate) neuron (cell 79-7) in cat central nucleus (ICC), illustrated in the sagittal plane. The dendrites are omitted to show axonal arbors clearly. The main axon (*arrowhead*) coursed laterally toward the brachium of the IC, local axon collaterals were widely distributed in the IC, and over 2000 terminal boutons were found. It appears that the axonal arborization is not restricted to a particular lamina (*D*, dorsal; *R*, rostral) (S*cale bar:* 500 μm). **(B)** The axons and dendrites of flat (411L) and less-flat (969L) neurons. Dendritic trees and axons are shown in *red* and *black*, respectively, and loci of cell bodies are indicated by *arrows*. Laminar axonal plexuses are clearly seen in the frontal view. Intralaminar arborization is apparent (*top view*): 411L has an extensive plexus, 969L has a smaller one and has a projection axon entering the brachium of the IC (*arrowheads*). The CFs of 411L and 969L are 4.9 and 5.1 kHz, respectively (s*cale bar:* 1 mm). **(C)** The axon of a glutamatergic neuron (cell 10-95) with oriented dendrites. This neuron makes axosomatic contacts on 30 large GABAergic neurons (*dot*s) (*scale bar:* 250 μm). [**A** was kindly provided by Dr. Douglas L. Oliver, from Oliver et al. (1991) with permission from Wiley; **B** was modified from Wallace et al. (2012), kindly provided by Dr. Mark N. Wallace; **C** was modified from Ito and Oliver (2014) with permission from Wiley]

purely interneurons. In a juxtacellular study, the authors also suggested the presence of interneurons in the ICC (e.g., cell 411L in Fig. 6.8B) (Wallace et al. 2012). These studies clearly showed that many IC neurons give rise to local collaterals with numerous boutons, and, therefore, they may influence many other adjacent neurons.

Since IC neurons outnumber the total number of all lower brainstem auditory nuclei (Kulesza et al. 2002), it is likely that the local collaterals are among the largest sources of inputs to the IC, and they may act as input amplifiers. Such massive local inputs undoubtedly exert a key influence in shaping de novo responses to sound. A wide variety of arborization patterns of axon collaterals have been reported (Fig. 6.8A–C), so the role of local neurons within a synaptic domain may also be very diverse. For example, large stellate neurons with extensive, unoriented axonal terminations and numerous boutons (Fig. 6.8A) may influence multiple synaptic domains in multiple isofrequency laminae. Laminar neurons (Fig. 6.8B, C) are more likely to exert their influence in the single lamina in which their cell bodies lie, although the area under influence may differ among neurons. Indeed, a functional imaging study on IC slices (Chandrasekaran et al. 2013) showed both cross-laminar and intra-laminar activity elicited by electrical stimulation. Unoriented axonal terminations in multiple laminae are ideal for causing the cross-laminar activity, which may affect spectral integration. These authors also demonstrated that repetitive stimulation in laminar slices (which in theory preserves local circuitry in a single lamina) resulted in the emergence of domains of high activity, which may reflect anatomical synaptic domains. Focal application of concentrated divalent cations, which causes inhibition of local circuit activity (Sivaramakrishnan et al. 2013), narrowed the dynamic range for sound intensity, suggesting that local circuits also affect encoding sound intensity (Grimsley et al. 2013).

6.5.3 Roles of GABAergic Cells

Neurotransmission of GABA plays an important role in IC function, both in the intrinsic circuitry and in the projections to the MGB. Two types of GABAergic neurons have been identified (Ito et al. 2009). The large and small GABAergic neurons differ in their synaptic organization, and both types are randomly distributed within the ICC (Fig. 6.5D) such that each type of synaptic domain may contain these two types of neurons in addition to glutamatergic neurons (Ito and Oliver 2012). The LG neurons receive dense excitatory axosomatic inputs (Ito et al. 2009). The excitatory terminals are positive for VGLUT2 but not VGLUT1 (Ito et al. 2009) and originate from the IC, INLL, SOC, and DCN (Ito and Oliver 2014; Ito et al. 2015). In all of those sites, the majority of IC-projecting glutamatergic neurons express VGLUT2 but not VGLUT1 (Ito and Oliver 2010; Ito et al. 2011). Since a single axon makes only a few (1–7) axosomatic terminals, many excitatory neurons may converge on the cell body of a single LG neuron (Ito and Oliver 2014; Ito et al. 2015). In addition, intrinsic glutamatergic neurons make axosomatic contacts on many nearby LG neurons (Fig. 6.8C).

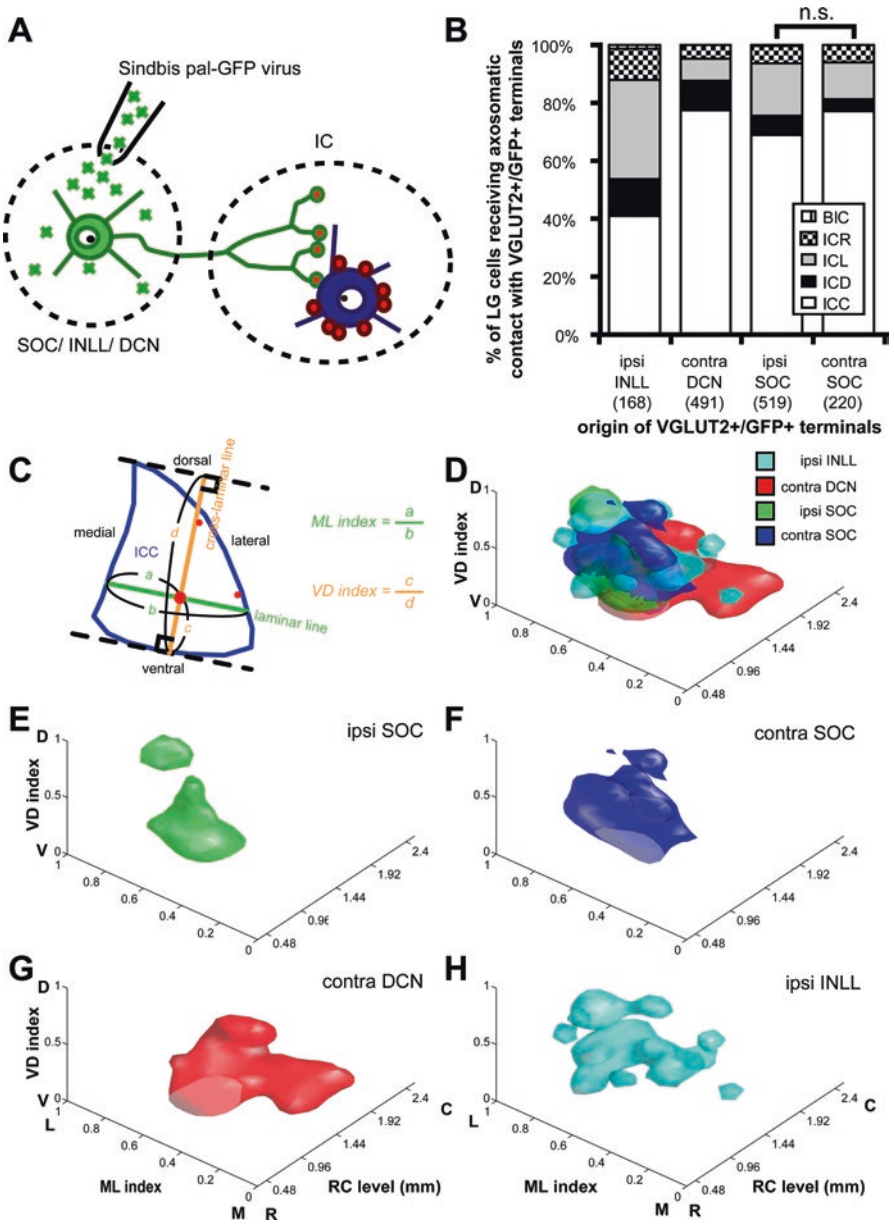

Fig. 6.9 Neurons in a particular lower auditory brain stem nucleus make axosomatic contacts on large GABAergic (LG) neurons in a particular region of the inferior colliculus (IC). **(A)** Schematic drawing of the experiment (Ito and Oliver 2014; Ito et al. 2015): an injection of Sindbis pal-GFP virus was made in either the superior olivary complex (*SOC*), dorsal cochlear nucleus (*DCN*), or intermediate nucleus of the lateral lemniscus (*INLL*), and the distribution of LG neurons that received axosomatic contacts with axons from GFP-expressing excitatory (GFP+/VGLUT2) neurons was examined. **(B)** The proportion of LG neurons receiving axosomatic contact with GFP+/VGLUT2+ terminals in each IC subdivision is different among the origins of GFP+ axons

Within each IC subdivision, the distribution of excitatory axosomatic terminals on LG neurons differs, depending on which brain stem nucleus is the source of input (Ito et al. 2015). Excitatory neurons in the DCN and SOC mainly target LG cells in the ICC, whereas those in the INLL target cortices of the IC as well as the ICC. After an injection of Sindbis pal-GFP virus in either DCN or SOC (Fig. 6.9A), the majority of LG neurons that receive labeled axosomatic contacts is located in the ICC, but less than half is located in the ICC in the INLL injection cases (Fig. 6.9B). The percentage of LG neurons receiving labeled axosomatic contacts in each subdivision was significantly different among the source nuclei except for the ipsilateral versus contralateral SOCs (Fig. 6.9B).

Even within the ICC, the spatial distribution of LG cells that receive axosomatic contacts from identified sources differs according to the nucleus of origin. SOC glutamatergic axons made contacts on LG cells mainly in the lateral part of the ICC, while DCN axons made contacts on LG cells mostly in the caudal and ventral parts. LG cells receiving axosomatic contacts with INLL terminals were sparsely distributed within the ICC. To quantify the distribution of LG neurons in ICC that received inputs from a particular source, the mediolateral (ML) and ventrodorsal (VD) position was calculated for all LG cells receiving particular inputs (Fig. 6.9C). The quantitative results are consistent with the conclusion that LG cells in different IC locations tend to receive axosomatic inputs from different sources. The spatial distribution of these LG neurons is illustrated in Fig. 6.9D–H in three-dimensional surface plots. In the plots, three-dimensional histograms of the LG neuron distribution were calculated (dimension was 9 × 11 × 11 on ML, VD indices, and rostrocaudal (RC) level axes, respectively) and histogram blocks that contain more LG neurons (>0.5% of all LG cells counted) were visualized. Each plot represents an ICC region that contains more LG neurons receiving axosomatic contact from a given source than the region outside. The axons from the contralateral DCN mainly made axosomatic contacts on LG cells located in the ventral and caudal part of the ICC (Fig. 6.9D, G), while SOC axons mainly terminated on LG cells in the rostral and lateral part (Fig. 6.9D–F). The region receiving INLL axons extended to the dorsal and rostral part of the ICC (Fig. 6.9D, H). Although these regions overlapped, the shape of the distributions was significantly different with the exception of the contralateral SOC versus the ipsilateral INLL and the ipsilateral versus contralateral

Fig. 6.9 (continued) (DCN, SOC, or INLL). *Numbers in parentheses* indicate the number of LG neurons with contact. Statistical significance (contralateral DCN vs. contralateral SOC, P = 0.019; other pairs, P < 0.001) was detected between nuclei of origin except for ipsilateral SOC versus contralateral SOC (P = 0.146; pairwise comparisons using Fisher's exact test). **(C)** A schematic diagram of ML and VD indices. For each LG neuron in the ICC, a line passing through the cell body and parallel to the most ventral lamina of the ICC (*laminar line segment*) is drawn. The *ML index* reflects mediolateral location of the LG cell. The *VD index* reflects relative ventrodorsal location of an LG cell in ICC. This is the position of an LG cell on a cross-laminar line orthogonal to the laminar line. The RC position of an LG cell was measured from the rostral end of the ICC. **(D–H)** Three-dimensional surface plots showing ICC zones of LG cells receiving axosomatic contact from ipsilateral SOC (**D, E**), contralateral SOC (**D, F**), contralateral DCN (**D, G**), and ipsilateral INLL (**D, H**). (*C*, caudal; *L*, lateral; *M*, medial; *R*, rostral)

SOCs. Thus, the LG neurons in an ICC synaptic domain mix particular excitatory ascending inputs with local IC inputs. The local inputs could be from another domain on the same lamina that received a different ascending input. Further, since LG neurons most likely have a stellate dendritic morphology (Oliver et al. 1994), they may also integrate spectral information across laminae.

Both GABAergic and glutamatergic IC neurons project to the MGB (Bartlett and Smith 1999). In rodents, feedforward inhibition by IC GABAergic neurons may be especially important because GABAergic interneurons are virtually absent in the medial geniculate (Winer et al. 1996; Ito et al. 2011). It is highly likely that the main source of feedforward GABAergic inputs in the MGV is LG neurons because most of the GABAergic neurons in the ICC that project to the MGB are LG neurons (Ito et al. 2009), but SG neurons in the IC cortices may also project to the thalamus since neurons in layer 2, which are made of GABA modules, project to the suprageniculate nucleus (Linke 1999).

LG neurons terminate on specific neuron types of the MGB. Inhibitory synapses of IC axons are small and terminate both on cell bodies and higher order dendritic branches of MGB neurons, while excitatory synapses of IC axons vary in size and terminate more widely on dendrites (Bartlett et al. 2000). In vitro studies in slice preparations have shown that electrical shock on the brachium of the IC stimulates ascending fibers from the IC and produces postsynaptic potentials in MGB neurons. An IPSP is evoked in stellate neurons in the dorsal division of the MGB (the MGD) and a subpopulation of tufted neurons in MGV and MGD (Bartlett and Smith 1999). During development, the IPSPs elicited by similar electrical shocks of the brachium show increasing intensity, shortened latencies, and reduced depression of responses (Venkataraman and Bartlett 2013). Mature LG neurons may make secure synapses that control the rising phase of excitation. Indeed, GABAergic axons have the largest diameters among brachial axons and are especially suitable for rapid transmission of action potentials (Saint Marie et al. 1997). Furthermore, at postnatal day 27, 40% of MGB neurons exhibit purely inhibitory responses to shock of the brachium (Venkataraman and Bartlett 2013). It is possible that the main drivers of these MGB neurons are corticothalamic descending fibers, while ascending sensory inputs from LG neurons block their activity.

6.6 Efferent Projections of Neurons in the Inferior Colliculus

6.6.1 Ascending Projections

Since the details of organization of the tectothalamic projection are described by Cant and Oliver (Chap. 2), the following section summarizes only the major differences in the main targets of the ICC and IC cortex. Most ICC neurons are projection

neurons (at least 80% of cat ICC neurons) (Oliver 1984), and their main targets are the MGV and the medial division of MGB (the MGM) (LeDoux et al. 1985).

In the IC cortex, the outer layers (layers 1 and 2) in ICL and ICD share similar inputs and outputs (Herbert et al. 1991; Linke 1999), suggesting that they serve a similar function. Layer 1 neurons project to the posterior intralaminar and peripeduncular nucleus (Linke 1999). Layer 2 neurons project to the suprageniculate nucleus in the thalamus (Linke 1999). In rats, ICL layer 3 neurons project to the MGM (Linke 1999). In cats, the ICD deep layer projects to the MGD (Kudo and Niimi 1980). All the targets of the IC cortex are considered to be multimodal nuclei.

6.6.2 Commissural Connections

A large number of neurons interconnect the two ICs through the commissure of the IC (the CoIC) (Okoyama et al. 2006; Malmierca et al. 2009). Neurons that give rise to uniquely commissural projections may be rare since González-Hernández et al. (1986) have shown that the majority of cells that project to the ipsilateral medial geniculate body also send collaterals to the contralateral IC.

Small injections of tracers into an isofrequency lamina of the ICC label fibers in the corresponding lamina on the contralateral side (Saldaña and Merchán 1992), indicating connections between the homotopic isofrequency lamina on the two sides. However, the density of these projections is biased toward a point that matches the position of the tracer injection (Fig. 6.10), which is consistent with a point-to-point emphasis in the wiring pattern of commissural fibers (Malmierca et al. 2009). At least some ICD neurons make laminar terminations in the contralateral ICC and ICD (Fig. 6.10), whereas ICL neurons do not form laminar plexuses and terminate mainly in the contralateral ICD and ICL (Saldaña and Merchán 2005). Recent electrophysiological studies demonstrated that commissural connections modulate the spectral, temporal, and binaural properties of many IC neurons (Malmierca et al. 2003, 2005). More recent experiments using the cooling technique have demonstrated that mostly non-Vshaped frequency response areas in the IC are modulated by the contralateral IC. Moreover, the supra-threshold sensitivity of rate-level functions decreases during deactivation, and the ability to signal changes in sound level is diminished. This commissural enhancement suggests the ICs should be viewed as a single entity in which the representation of sound in each is governed by the other (Orton and Rees 2014). A large proportion of neurons contributing to the commissural projection may be glutamatergic, as in guinea pig (Saint Marie 1996), and about 20% of the neurons in rat are GABAergic (Hernández et al. 2006). These neurochemical properties are consistent with physiological studies that show that the commissural inputs may have either an excitatory or inhibitory influence on neurons in the contralateral IC (in vitro, guinea pig: Smith 1992; Li et al. 1998; in vivo, rat: Malmierca et al. 2003, 2005).

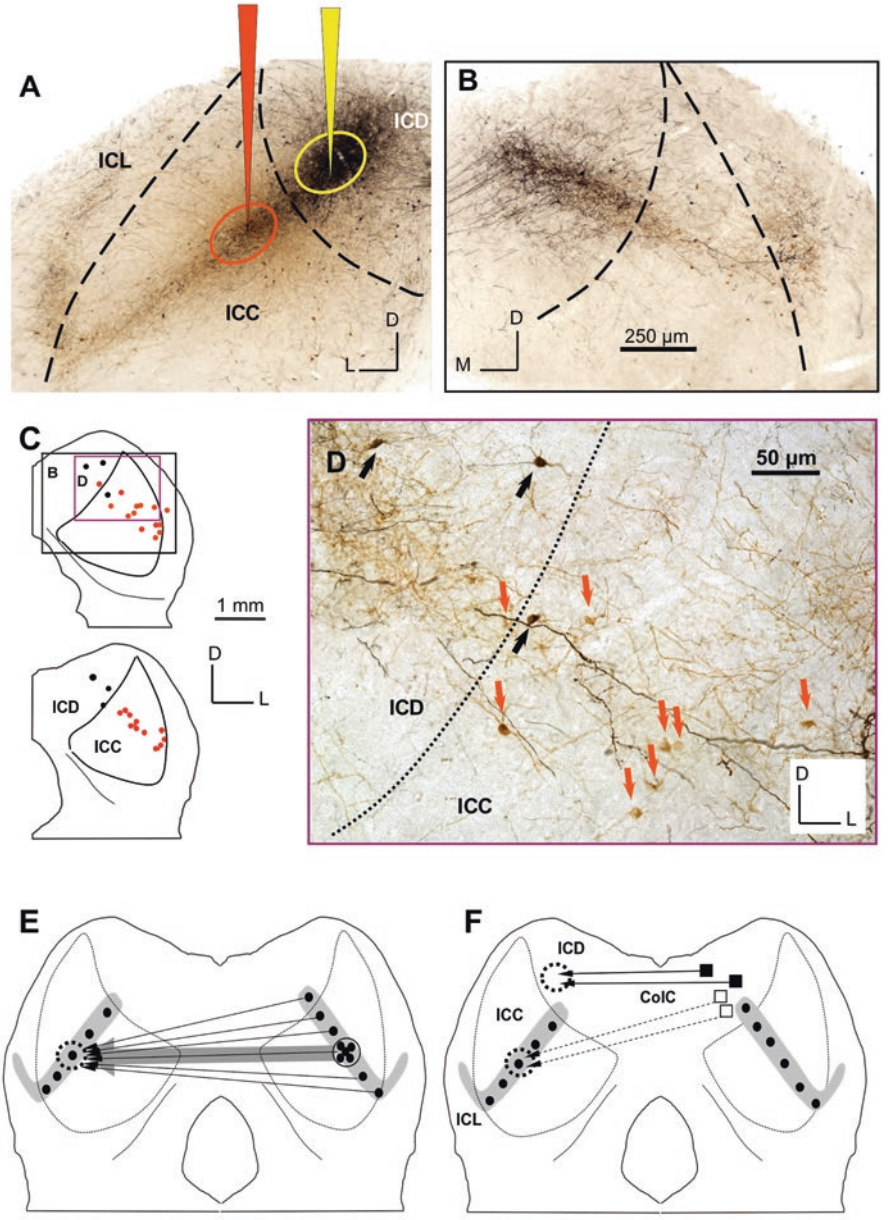

Fig. 6.10 **(A)** A photomicrograph showing two injections into the same lamina of the inferior colliculus (IC) (case # 279 in Malmierca et al. 2005). An injection (FD-BDA, *yellow circle*) was confined to the dorsal IC (*ICD*); another injection (tetramethylrhodamine dextran, TRD, *orange circle*) was located at the central nucleus (*ICC*). The characteristic frequency (CF) at the injection sites was similar and within the same laminae (10–10.5 kHz). Note the typical V-shaped or wing-like plexus of intrinsic axons with a central wing that extends into the ICC (described by Saldaña and Merchán 1992) and a lateral wing located in the lateral IC (*ICL*). The vertex of the plexus

6.6.3 Descending Projections

In addition to the thalamic projections, the IC also gives rise to colliculo-lemniscal, colliculo-olivary, and colliculo-cochlear projections (Caicedo and Herbert 1993). The colliculo-lemniscal projections are largely restricted to the DNLL, the sagulum, the horizontal cell group, and the perilemniscal zone (Caicedo and Herbert 1993). The colliculo-olivary projections originate in the ICC, ICL, and ICR and terminate as bands of terminals that target the rostral and medioventral periolivary nuclei (Caicedo and Herbert 1993). This projection is tonotopic and the axonal fields terminate at the site of origin of the medial olivocochlear system (White and Warr 1983), suggesting that the IC modulates cochlear activity. The classical electrophysiological studies by Dolan and Nuttall (1988) in guinea pigs and by Rajan (1990) in cats support this notion. The colliculo-cochlear projection originates in the ICC and ICL and targets the DCN and granule cell domain of the VCN (Caicedo and Herbert 1993), but the functional roles of these projections are still unknown.

Finally, it is interesting to note that the IC also projects to nonauditory areas, including the pontine nuclei, the lateral paragigantocellular nucleus, the gigantocellular reticular nucleus, the ventrolateral tegmental nucleus, and the caudal pontine reticular nucleus (Caicedo and Herbert 1993). These nuclei also receive strong projections from the CN (Kandler and Herbert 1991). These nonauditory areas may play a role in acoustically elicited autonomic responses or long- and short-latency auditory–motor behaviors (Kandler and Herbert 1991; Caicedo and Herbert 1993).

Fig. 6.10 (continued) marks the border between the ICC and the ICL. **(B)** Anterogradely labeled axons and retrogradely labeled neurons on the side contralateral to the injections in **A**. **(C)** Camera lucida drawings of the retrogradely labeled neurons originating from the TRD (*orange*) and mixture of fluorescein dextran and biotinylated dextran amine (FD-BDA) (*black*) injections at two rostrocaudal levels of the IC. *Black box* in the most caudal section highlights area shown in **B** and the *purple box* highlights area shown in **D** at higher magnification. **(D)** Area in *purple box* in **C***;* the *orange arrows* point to TRD-labeled neurons and *black arrows* FD-BDA-labeled neurons. **(E, F)** Schematic wiring diagrams of the commissural connections; *filled circles* are somata and *dotted circles* indicate that an injection into one point on the lamina (e.g., dotted circle, left IC) retrogradely labels neurons over the whole extent of the contralateral lamina, consistent with a divergent pattern of connections (*thin arrows*). **(E)** In the ICC, anterograde labeling and the retrograde labeling of neurons also support a convergent projection. In addition, however, the density of the projection is centered on a point matching the position of the tracer injection. This result is consistent with a point-to-point weighted-wiring pattern (*thick arrow*). The coexistence of convergent and point-to-point projections suggests that there are two functionally different systems of commissural connections (*CoIC*). **(F)** In the dorsal IC (*ICD*), two populations of neurons seem to contribute to the commissural projections to the contralateral IC: one ICD population projects to the frequency-band laminae in the ICC in a tonotopic manner (*white squares, dashed lines*), while the other ICD population projects diffusely to its counterpart (*black squares, solid lines*). (*C*, caudal; *D*, dorsal; *L*, lateral; *R*, rostral) (*Scale bars* as labeled in **B**, **C**, **D**)

6.7 Summary

The IC is subdivided into the ICC and surrounding cortices. The ICC is characterized by the presence of fibrodendritic laminae that are composed of oriented axons from lemniscal nuclei and the dendritic arbors of flat neurons. IC cortices, especially ICL, are organized in several layers. Since different layers receive different combinations of sensory modal inputs, the IC cortex may be involved in multimodal integration.

Various neuron types have been identified in the IC. Different types of dendritic arborizations may reflect different degrees of frequency integration in the ICC and multisensory integration in the IC cortex. Some GABAergic neurons can be linked to specific functions. Although there is diversity in the intrinsic properties of IC neurons, the proportion of each neuron type classified with intrinsic properties is different among subdivisions. There is also wide diversity of sound-evoked activity in the IC. The IC cortex can be characterized by the presence of neurons showing SSA. These neuron types successfully distinguish IC subdivisions.

Lower brain stem auditory nuclei (e.g., CN, SOC, and NLL) mainly target the ICC, while AC axons mainly target the IC cortex (although A1 also targets the ICC). The ICC and ICD neurons form a laminar axonal plexus in both ICs. The ICL neurons terminate bilaterally in ICD and ICL in a nonlaminar pattern. These data clearly indicate the different combinations of inputs in different subdivisions of the IC.

Within a subdivision, there are synaptic domains that receive different combinations of inputs. In the ICC, LG neurons may mix information from multiple synaptic domains via collaterals of excitatory neurons located in neighboring domains. Taken together, it is plausible to conclude that microcircuits in the ICC are especially suited to integrate ascending auditory information and create de novo coding properties, whereas microcircuits of the IC cortex are more suitable for integrating multimodal information and detecting novel features of a stimulus.

Acknowledgments The authors are grateful to Drs. Douglas L. Oliver, Munenori Ono, and Mark N. Wallace for providing excellent images. Financial support was provided by the Spanish Ministerio de Economía y Competitividad (SAF2016-75803-P) and Consejeria de Educación JCYL grant (SA343U14) to MSM; support was provided by Japan Society for the Promotion of Science (KAKENHI Grant numbers: 16H01501, 16K07026, 22700365, and 25430034), the Uehara Memorial Foundation, the Ichiro Kanehara Foundation, Novartis Foundation of Japan, Takahashi Industrial and Economic Research Foundation, and Research and Education Program for Life Science of University of Fukui to TI.

Compliance with Ethics Requirements Tetsufumi Ito declares no conflicts of interest.

Manuel S. Malmierca declares no conflicts of interest.

References

Ahuja, T. K., & Wu, S. H. (2007). Intrinsic membrane properties and synaptic response characteristics of neurons in the rat's external cortex of the inferior colliculus. *Neuroscience, 145*(3), 851–865.

Anderson, L. A., & Malmierca, M. S. (2013). The effect of auditory cortex deactivation on stimulus-specific adaptation in the inferior colliculus of the rat. *European Journal of Neuroscience, 37*(1), 52–62.

Aubrey, K. R., Rossi, F. M., Ruivo, R., Alboni, S., Bellenchi, G. C., Le Goff, A., et al. (2007). The transporters GlyT2 and VIAAT cooperate to determine the vesicular glycinergic phenotype. *The Journal of Neuroscience, 27*(23), 6273–6281.

Ayala, Y. A., & Malmierca, M. S. (2012). Stimulus-specific adaptation and deviance detection in the inferior colliculus. *Frontiers in Neural Circuits, 6*, 89. https://doi.org/10.3389/fncir.2012.00089.

Ayala, Y. A., & Malmierca, M. S. (2015). Cholinergic modulation of stimulus-specific adaptation in the inferior colliculus. *The Journal of Neuroscience, 35*(35), 12261–12272.

Ayala, Y. A., Udeh, A., Dutta, K., Bishop, D., Malmierca, M. S., & Oliver, D. L. (2015). Differences in the strength of cortical and brainstem inputs to SSA and non-SSA neurons in the inferior colliculus. *Scientific Reports, 5*, 10383. https://doi.org/10.1038/srep10383.

Bartlett, E. L., & Smith, P. H. (1999). Anatomic, intrinsic, and synaptic properties of dorsal and ventral division neurons in rat medial geniculate body. *Journal of Neurophysiology, 81*(5), 1999–2016.

Bartlett, E. L., Stark, J. M., Guillery, R. W., & Smith, P. H. (2000). Comparison of the fine structure of cortical and collicular terminals in the rat medial geniculate body. *Neuroscience, 100*(4), 811–828.

Caicedo, A., & Herbert, H. (1993). Topography of descending projections from the inferior colliculus to auditory brainstem nuclei in the rat. *The Journal of Comparative Neurology, 328*(3), 377–392.

Cant, N. B., & Benson, C. G. (2006). Organization of the inferior colliculus of the gerbil (*Meriones unguiculatus*): Differences in distribution of projections from the cochlear nuclei and the superior olivary complex. *The Journal of Comparative Neurology, 495*(5), 511–528.

Cant, N. B., & Benson, C. G. (2007). Multiple topographically organized projections connect the central nucleus of the inferior colliculus to the ventral division of the medial geniculate nucleus in the gerbil, *Meriones unguiculatus*. *The Journal of Comparative Neurology, 503*(3), 432–453.

Casseday, J. H., Fremouw, T., & Covey, E. (2002). The inferior colliculus: A hub for the central auditory system. In D. Oertel, R. R. Fay, & A. N. Popper (Eds.), *Integrative functions in the mammalian auditory pathway* (pp. 238–318). New York: Springer.

Chandrasekaran, L., Xiao, Y., & Sivaramakrishnan, S. (2013). Functional architecture of the inferior colliculus revealed with voltage-sensitive dyes. *Frontiers in Neural Circuits, 7*, 41. https://doi.org/10.3389/fncir.2013.00041.

Chen, C., Rodriguez, F. C., Read, H. L., & Escabi, M. A. (2012). Spectrotemporal sound preferences of neighboring inferior colliculus neurons: Implications for local circuitry and processing. *Frontiers in Neural Circuits, 6*, 62. https://doi.org/10.3389/fncir.2012.00062.

Chernock, M. L., Larue, D. T., & Winer, J. A. (2004). A periodic network of neurochemical modules in the inferior colliculus. *Hearing Research, 188*(1-2), 12–20.

Coleman, J. R., & Clerici, W. J. (1987). Sources of projections to subdivisions of the inferior colliculus in the rat. *The Journal of Comparative Neurology, 262*(2), 215–226.

Coote, E. J., & Rees, A. (2008). The distribution of nitric oxide synthase in the inferior colliculus of guinea pig. *Neuroscience, 154*(1), 218–225.

Covey, E., & Carr, C. E. (2005). The auditory midbrain in bats and birds. In J. A. Winer & C. E. Schreiner (Eds.), *The inferior colliculus* (pp. 493–536). New York: Springer.

Dolan, D. F., & Nuttall, A. L. (1988). Masked cochlear whole-nerve response intensity functions altered by electrical stimulation of the crossed olivocochlear bundle. *Journal of the Acoustical Society of America, 83*(3), 1081–1086.

Duque, D., Perez-Gonzalez, D., Ayala, Y. A., Palmer, A. R., & Malmierca, M. S. (2012). Topographic distribution, frequency, and intensity dependence of stimulus-specific adaptation in the inferior colliculus of the rat. *The Journal of Neuroscience, 32*(49), 17762–17774.

Faingold, C. L., Gehlbach, G., & Caspary, D. M. (1989). On the role of GABA as an inhibitory neurotransmitter in inferior colliculus neurons: Iontophoretic studies. *Brain Research, 500*(1-2), 302–312.

Faingold, C. L., Boersma Anderson, C. A., & Caspary, D. M. (1991). Involvement of GABA in acoustically evoked inhibition in inferior colliculus neurons. *Hearing Research, 52*(1), 201–216.

Faye-Lund, H., & Osen, K. K. (1985). Anatomy of the inferior colliculus in rat. *Anatomy and Embryology (Berlin), 171*(1), 1–20.

Fremeau, R. T., Jr., Troyer, M. D., Pahner, I., Nygaard, G. O., Tran, C. H., Reimer, R. J., Bellocchio, E. E., Fortin, D., Storm-Mathisen, J., & Edwards, R. H. (2001). The expression of vesicular glutamate transporters defines two classes of excitatory synapse. *Neuron, 31*(2), 247–260.

Games, K. D., & Winer, J. A. (1988). Layer V in rat auditory cortex: Projections to the inferior colliculus and contralateral cortex. *Hearing Research, 34*(1), 1–25.

Geis, H. R., & Borst, J. G. (2013). Large GABAergic neurons form a distinct subclass within the mouse dorsal cortex of the inferior colliculus with respect to intrinsic properties, synaptic inputs, sound responses, and projections. *The Journal of Comparative Neurology, 521*(1), 189–202.

González-Hernández, T. H., Meyer, G., & Ferres-Torres, R. (1986). The commissural interconnections of the inferior colliculus in the albino mouse. *Brain Research, 368*(2), 268–276.

Grimsley, C. A., Sanchez, J. T., & Sivaramakrishnan, S. (2013). Midbrain local circuits shape sound intensity codes. *Frontiers in Neural Circuits, 7*, 174. https://doi.org/10.3389/fncir.2013.00174.

Gruters, K. G., & Groh, J. M. (2012). Sounds and beyond: Multisensory and other non-auditory signals in the inferior colliculus. *Frontiers in Neural Circuits, 6*, 96. https://doi.org/10.3389/fncir.2012.00096.

Henderson, Z., & Sherriff, F. E. (1991). Distribution of choline acetyltransferase immunoreactive axons and terminals in the rat and ferret brainstem. *The Journal of Comparative Neurology, 314*(1), 147–163.

Herbert, H., Aschoff, A., & Ostwald, J. (1991). Topography of projections from the auditory cortex to the inferior colliculus in the rat. *The Journal of Comparative Neurology, 304*(1), 103–122.

Hernández, O., Rees, A., & Malmierca, M. S. (2006). A GABAergic component in the commissure of the inferior colliculus in rat. *Neuroreport, 17*(15), 1611–1614.

Hu, B., Senatorov, V., & Mooney, D. (1994). Lemniscal and non-lemniscal synaptic transmission in rat auditory thalamus. *The Journal of Physiology, 479*(2), 217–231.

Itaya, S. K., & Van Hoesen, G. W. (1982). Retinal innervation of the inferior colliculus in rat and monkey. *Brain Research, 233*(1), 45–52.

Ito, T., & Oliver, D. L. (2010). Origins of glutamatergic terminals in the inferior colliculus identified by retrograde transport and expression of VGLUT1 and VGLUT2 genes. *Frontiers in Neuroanatomy, 4*, 135. https://doi.org/10.3389/fnana.2010.00135.

Ito, T., & Oliver, D. L. (2012). The basic circuit of the IC: Tectothalamic neurons with different patterns of synaptic organization send different messages to the thalamus. *Frontiers in Neural Circuits, 6*, 48. https://doi.org/10.3389/fncir.2012.00048.

Ito, T., & Oliver, D. L. (2014). Local and commissural IC neurons make axosomatic inputs on large GABAergic tectothalamic neurons. *The Journal of Comparative Neurology, 522*(15), 3539–3554.

Ito, T., Hioki, H., Nakamura, K., Tanaka, Y., Nakade, H., Kaneko, T., Iino, S., & Nojyo, Y. (2007). Gamma-aminobutyric acid-containing sympathetic preganglionic neurons in rat thoracic spinal

cord send their axons to the superior cervical ganglion. *The Journal of Comparative Neurology, 502*(1), 113–125.

Ito, T., Bishop, D. C., & Oliver, D. L. (2009). Two classes of GABAergic neurons in the inferior colliculus. *The Journal of Neuroscience, 29*(44), 13860–13869.

Ito, T., Bishop, D. C., & Oliver, D. L. (2011). Expression of glutamate and inhibitory amino acid vesicular transporters in the rodent auditory brainstem. *The Journal of Comparative Neurology, 519*(2), 316–340.

Ito, T., Hioki, H., Sohn, J., Okamoto, S., Kaneko, T., Iino, S., & Oliver, D. L. (2015). Convergence of lemniscal and local excitatory inputs on large GABAergic tectothalamic neurons. *The Journal of Comparative Neurology, 523*, 2277–2296.

Joris, P. X., & Yin, T. C. (1995). Envelope coding in the lateral superior olive. I. Sensitivity to interaural time differences. *Journal of Neurophysiology, 73*(3), 1043–1062.

Kandler, K., & Herbert, H. (1991). Auditory projections from the cochlear nucleus to pontine and mesencephalic reticular nuclei in the rat. *Brain Research, 562*(2), 230–242.

Klepper, A., & Herbert, H. (1991). Distribution and origin of noradrenergic and serotonergic fibers in the cochlear nucleus and inferior colliculus of the rat. *Brain Research, 557*(1-2), 190–201.

Kudo, M., & Niimi, K. (1980). Ascending projections of the inferior colliculus in the cat: An autoradiographic study. *The Journal of Comparative Neurology, 191*(4), 545–556.

Kulesza, R. J., Vinuela, A., Saldana, E., & Berrebi, A. S. (2002). Unbiased stereological estimates of neuron number in subcortical auditory nuclei of the rat. *Hearing Research, 168*(1-2), 12–24.

Kuo, R. I., & Wu, G. K. (2012). The generation of direction selectivity in the auditory system. *Neuron, 73*(5), 1016–1027.

Kuwada, S., Batra, R., Yin, T. C. T., Oliver, D. L., Haberly, L. B., & Stanford, T. R. (1997). Intracellular recordings in response to monaural and binaural stimulation of neurons in the inferior colliculus of the cat. *The Journal of Neuroscience, 17*(19), 7565–7581.

LeDoux, J. E., Ruggiero, D. A., & Reis, D. J. (1985). Projections to the subcortical forebrain from anatomically defined regions of the medial geniculate body in the rat. *The Journal of Comparative Neurology, 242*(2), 182–213.

Lesicko, A., & Llano, D. (2015). Connectional and neurochemical modularity of the mouse inferior colliculus. Abstract PS-564, Association for Research in Otolaryngology Midwinter Meeting, February 21–25, Baltimore, MD.

Li, Y., Evans, M. S., & Faingold, C. L. (1998). In vitro electrophysiology of neurons in subnuclei of rat inferior colliculus. *Hearing Research, 121*(1-2), 1–10.

Linke, R. (1999). Differential projection patterns of superior and inferior collicular neurons onto posterior paralaminar nuclei of the thalamus surrounding the medial geniculate body in the rat. *European Journal of Neuroscience, 11*(1), 187–203.

Loftus, W. C., Bishop, D. C., Saint Marie, R. L., & Oliver, D. L. (2004). Organization of binaural excitatory and inhibitory inputs to the inferior colliculus from the superior olive. *The Journal of Comparative Neurology, 472*(3), 330–344.

Loftus, W. C., Bishop, D. C., & Oliver, D. L. (2010). Differential patterns of inputs create functional zones in central nucleus of inferior colliculus. *The Journal of Neuroscience, 30*(40), 13396–13408.

Loftus, W. C., Malmierca, M. S., Bishop, D. C., & Oliver, D. L. (2008). The cytoarchitecture of the inferior colliculus revisited: A common organization of the lateral cortex in rat and cat. *Neuroscience, 154*(1), 196–205.

Malmierca, M. S. (2015). Auditory system. In G. Paxinos (Ed.), *The rat nervous system* (4th ed., pp. 865–946). Amsterdam: Academic Press.

Malmierca, M. S., & Ryugo, D. K. (2011). Descending connections of auditory cortex to the midbrain and brainstem. In J. A. Winer & C. E. Schreiner (Eds.), *The auditory cortex* (pp. 189–208). New York: Springer.

Malmierca, M. S., Blackstad, T. W., Osen, K. K., Karagulle, T., & Molowny, R. L. (1993). The central nucleus of the inferior colliculus in rat: A Golgi and computer reconstruction study of neuronal and laminar structure. *The Journal of Comparative Neurology, 333*(1), 1–27.

Malmierca, M. S., Rees, A., Le Beau, F. E., & Bjaalie, J. G. (1995). Laminar organization of frequency-defined local axons within and between the inferior colliculi of the guinea pig. *The Journal of Comparative Neurology, 357*(1), 124–144.

Malmierca, M. S., Hernández, O., Falconi, A., Lopez-Poveda, E. A., Merchán, M., & Rees, A. (2003). The commissure of the inferior colliculus shapes frequency response areas in rat: An in vivo study using reversible blockade with microinjection of kynurenic acid. *Experimental Brain Research, 153*(4), 522–529.

Malmierca, M. S., Hernández, O., & Rees, A. (2005). Intercollicular commissural projections modulate neuronal responses in the inferior colliculus. *European Journal of Neuroscience, 21*(10), 2701–2710.

Malmierca, M. S., Izquierdo, M. A., Cristaudo, S., Hernandez, O., Pérez-González, D., Covey, E., et al. (2008). A discontinuous tonotopic organization in the inferior colliculus of the rat. *The Journal of Neuroscience, 28*(18), 4767–4776.

Malmierca, M. S., Hernandez, O., Antunes, F. M., & Rees, A. (2009). Divergent and point-to-point connections in the commissural pathway between the inferior colliculi. *The Journal of Comparative Neurology, 514*(3), 226–239.

Malmierca, M. S., Blackstad, T. W., & Osen, K. K. (2011). Computer-assisted 3-D reconstructions of Golgi-impregnated neurons in the cortical regions of the inferior colliculus of rat. *Hearing Research, 274*(1-2), 13–26.

Matsuda, W., Furuta, T., Nakamura, K. C., Hioki, H., Fujiyama, F., Arai, R., et al. (2009). Single nigrostriatal dopaminergic neurons form widely spread and highly dense axonal arborizations in the neostriatum. *The Journal of Neuroscience, 29*(2), 444–453.

Merchán, M., Aguilar, L. A., Lopez-Poveda, E. A., & Malmierca, M. S. (2005). The inferior colliculus of the rat: Quantitative immunocytochemical study of GABA and glycine. *Neuroscience, 136*(3), 907–925.

Mitani, A., Shimokouchi, M., & Nomura, S. (1983). Effects of stimulation of the primary auditory cortex upon colliculogeniculate neurons in the inferior colliculus of the cat. *Neuroscience Letters, 42*(2), 185–189.

Moller, A. R., & Rees, A. (1986). Dynamic properties of the responses of single neurons in the inferior colliculus of the rat. *Hearing Research, 24*(3), 203–215.

Morest, D. K., & Oliver, D. L. (1984). The neuronal architecture of the inferior colliculus in the cat: Defining the functional anatomy of the auditory midbrain. *The Journal of Comparative Neurology, 222*(2), 209–236.

Motts, S. D., & Schofield, B. R. (2009). Sources of cholinergic input to the inferior colliculus. *Neuroscience, 160*(1), 103–114.

Nakagawa, H., Ikeda, M., Houtani, T., Ueyama, T., Baba, K., Kondoh, A., et al. (1995). Immunohistochemical evidence for enkephalin and neuropeptide Y in rat inferior colliculus neurons that provide ascending or commissural fibers. *Brain Research, 690*(2), 236–240.

Netser, S., Zahar, Y., & Gutfreund, Y. (2011). Stimulus-specific adaptation: Can it be a neural correlate of behavioral habituation? *The Journal of Neuroscience, 31*(49), 17811–17820.

Nwabueze-Ogbo, F. C., Popelar, J., & Syka, J. (2002). Changes in the acoustically evoked activity in the inferior colliculus of the rat after functional ablation of the auditory cortex. *Physiological Research, 51*(Supplement 1), 95–104.

Okoyama, S., Ohbayashi, M., Ito, M., & Harada, S. (2006). Neuronal organization of the rat inferior colliculus participating in four major auditory pathways. *Hearing Research, 218*(1-2), 72–80.

Oliver, D. L. (1984). Neuron types in the central nucleus of the inferior colliculus that project to the medial geniculate body. *Neuroscience, 11*(2), 409–424.

Oliver, D. L. (2005). Neuronal organization in the inferior colliculus. In J. A. Winer & C. E. Schreiner (Eds.), *The inferior colliculus* (pp. 69–114). New York: Springer.

Oliver, D. L., & Morest, D. K. (1984). The central nucleus of the inferior colliculus in the cat. *The Journal of Comparative Neurology, 222*(2), 237–264.

Oliver, D. L., & Huerta, M. F. (1992). Inferior and superior colliculi. In D. B. Webster, A. N. Popper, & R. R. Fay (Eds.), *The mammalian auditory pathway: Neuroanatomy* (pp. 168–221). New York: Springer.

Oliver, D. L., Kuwada, S., Yin, T. C., Haberly, L. B., & Henkel, C. K. (1991). Dendritic and axonal morphology of HRP-injected neurons in the inferior colliculus of the cat. *The Journal of Comparative Neurology, 303*(1), 75–100.

Oliver, D. L., Winer, J. A., Beckius, G. E., & Saint Marie, R. L. (1994). Morphology of GABAergic neurons in the inferior colliculus of the cat. *The Journal of Comparative Neurology, 340*(1), 27–42.

Oliver, D. L., Beckius, G. E., Bishop, D. C., & Kuwada, S. (1997). Simultaneous anterograde labeling of axonal layers from lateral superior olive and dorsal cochlear nucleus in the inferior colliculus of the cat. *The Journal of Comparative Neurology, 382*(2), 215–229.

Oliver, D. L., Beckius, G. E., Bishop, D. C., Loftus, W. C., & Batra, R. (2003). Topography of interaural temporal disparity coding in projections of medial superior olive to inferior colliculus. *The Journal of Neuroscience, 23*(19), 7438–7449.

Oliver, D. L., Izquierdo, M. A., & Malmierca, M. S. (2011). Persistent effects of early augmented acoustic environment on the auditory brainstem. *Neuroscience, 184*, 75–87.

Ono, M., Yanagawa, Y., & Koyano, K. (2005). GABAergic neurons in inferior colliculus of the GAD67-GFP knock-in mouse: Electrophysiological and morphological properties. *Neuroscience Research, 51*(4), 475–492.

Orton, L. D., & Rees, A. (2014). Intercollicular commissural connections refine the representation of sound frequency and level in the auditory midbrain. *eLife, 3*, e03764.

Palmer, A. R., Shackleton, T. M., Sumner, C. J., Zobay, O., & Rees, A. (2013). Classification of frequency response areas in the inferior colliculus reveals continua not discrete classes. *The Journal of Physiology, 591*(16), 4003–4025.

Pérez-González, D., Malmierca, M. S., & Covey, E. (2005). Novelty detector neurons in the mammalian auditory midbrain. *European Journal of Neuroscience, 22*(11), 2879–2885.

Pérez-González, D., Malmierca, M. S., Moore, J. M., Hernández, O., & Covey, E. (2006). Duration selective neurons in the inferior colliculus of the rat: Topographic distribution and relation of duration sensitivity to other response properties. *Journal of Neurophysiology, 95*(2), 823–836.

Pérez-González, D., Hernández, O., Covey, E., & Malmierca, M. S. (2012). $GABA_A$-mediated inhibition modulates stimulus-specific adaptation in the inferior colliculus. *PLoS One, 7*(3), e34297. https://doi.org/10.1371/journal.pone.0034297.

Peruzzi, D., Sivaramakrishnan, S., & Oliver, D. L. (2000). Identification of cell types in brain slices of the inferior colliculus. *Neuroscience, 101*(2), 403–416.

Poon, P. W., Chen, X., & Cheung, Y. M. (1992). Differences in FM response correlate with morphology of neurons in the rat inferior colliculus. *Experimental Brain Research, 91*(1), 94–104.

Rajan, R. (1990). Electrical stimulation of the inferior colliculus at low rates protects the cochlea from auditory desensitization. *Brain Research, 506*(2), 192–204.

Rees, A., & Moller, A. R. (1987). Stimulus properties influencing the responses of inferior colliculus neurons to amplitude-modulated sounds. *Hearing Research, 27*(2), 129–143.

Reetz, G., & Ehret, G. (1999). Inputs from three brainstem sources to identified neurons of the mouse inferior colliculus slice. *Brain Research, 816*(2), 527–543.

Saint Marie, R. L. (1996). Glutamatergic connections of the auditory midbrain: Selective uptake and axonal transport of D-[3H]aspartate. *The Journal of Comparative Neurology, 373*(2), 255–270.

Saint Marie, R. L., Stanforth, D. A., & Jubelier, E. M. (1997). Substrate for rapid feedforward inhibition of the auditory forebrain. *Brain Research, 765*(1), 173–176.

Saldaña, E., & Merchán, M. A. (1992). Intrinsic and commissural connections of the rat inferior colliculus. *The Journal of Comparative Neurology, 319*(3), 417–437.

Saldaña, E., & Merchán, M. A. (2005). Intrinsic and commissural connections of the inferior colliculus. In J. A. Winer & C. E. Schreiner (Eds.), *The inferior colliculus* (pp. 155–181). New York: Springer.

Saldaña, E., Feliciano, M., & Mugnaini, E. (1996). Distribution of descending projections from primary auditory neocortex to inferior colliculus mimics the topography of intracollicular projections. *The Journal of Comparative Neurology, 371*(1), 15–40.

Schreiner, C. E., & Langner, G. (1988). Periodicity coding in the inferior colliculus of the cat. II. Topographical organization. *Journal of Neurophysiology, 60*(6), 1823–1840.

Schreiner, C. E., & Langner, G. (1997). Laminar fine structure of frequency organization in auditory midbrain. *Nature, 388*(6640), 383–386.

Shammah-Lagnado, S. J., Alheid, G. F., & Heimer, L. (1996). Efferent connections of the caudal part of the globus pallidus in the rat. *The Journal of Comparative Neurology, 376*(3), 489–507.

Shera, C. A. (2015). The spiral staircase: Tonotopic microstructure and cochlear tuning. *The Journal of Neuroscience, 35*(11), 4683–4690.

Shneiderman, A., & Henkel, C. K. (1987). Banding of lateral superior olivary nucleus afferents in the inferior colliculus: A possible substrate for sensory integration. *The Journal of Comparative Neurology, 266*(4), 519–534.

Sivaramakrishnan, S., & Oliver, D. L. (2001). Distinct K currents result in physiologically distinct cell types in the inferior colliculus of the rat. *The Journal of Neuroscience, 21*(8), 2861–2877.

Sivaramakrishnan, S., Sanchez, J. T., & Grimsley, C. A. (2013). High concentrations of divalent cations isolate monosynaptic inputs from local circuits in the auditory midbrain. *Frontiers in Neural Circuits, 7*, 175. https://doi.org/10.3389/fncir.2013.00175.

Smith, P. H. (1992). Anatomy and physiology of multipolar cells in the rat inferior collicular cortex using the in vitro brain slice technique. *The Journal of Neuroscience, 12*(9), 3700–3715.

Sun, H., & Wu, S. H. (2008). Modification of membrane excitability of neurons in the rat's dorsal cortex of the inferior colliculus by preceding hyperpolarization. *Neuroscience, 154*(1), 257–272.

Tan, M. L., Theeuwes, H. P., Feenstra, L., & Borst, J. G. (2007). Membrane properties and firing patterns of inferior colliculus neurons: An in vivo patch-clamp study in rodents. *Journal of Neurophysiology, 98*(1), 443–453.

Tanaka, I., & Ezure, K. (2004). Overall distribution of GLYT2 mRNA-containing versus GAD67 mRNA-containing neurons and colocalization of both mRNAs in midbrain, pons, and cerebellum in rats. *Neuroscience Research, 49*(2), 165–178.

Tokunaga, A., Sugita, S., & Otani, K. (1984). Auditory and non-auditory subcortical afferents to the inferior colliculus in the rat. *Journal für Hirnforschung, 25*(4), 461–472.

Tongjaroenbuangam, W., Jongkamonwiwat, N., Phansuwan-Pujito, P., Casalotti, S. O., Forge, A., Dodson, H., et al. (2006). Relationship of opioid receptors with GABAergic neurons in the rat inferior colliculus. *European Journal of Neuroscience, 24*(7), 1987–1994.

Ulanovsky, N., Las, L., & Nelken, I. (2003). Processing of low-probability sounds by cortical neurons. *Nature Neuroscience, 6*(4), 391–398.

Venkataraman, Y., & Bartlett, E. L. (2013). Post-natal development of synaptic properties of the gabaergic projection from inferior colliculus to auditory thalamus. *Journal of Neurophysiology, 109*(12), 2866–2882.

Wallace, M. N., Shackleton, T. M., & Palmer, A. R. (2012). Morphological and physiological characteristics of laminar cells in the central nucleus of the inferior colliculus. *Frontiers in Neural Circuits, 6*, 55. https://doi.org/10.3389/fncir.2012.00055.

White, J. S., & Warr, W. B. (1983). The dual origins of the olivocochlear bundle in the albino rat. *The Journal of Comparative Neurology, 219*(2), 203–214.

Whitley, J. M., & Henkel, C. K. (1984). Topographical organization of the inferior collicular projection and other connections of the ventral nucleus of the lateral lemniscus in the cat. *The Journal of Comparative Neurology, 229*(2), 257–270.

Wiberg, M., Westman, J., & Blomqvist, A. (1987). Somatosensory projection to the mesencephalon: An anatomical study in the monkey. *The Journal of Comparative Neurology, 264*(1), 92–117.

Willard, F. H., & Ryugo, D. (1983). Anatomy of the central auditory system. In J. F. Willot (Ed.), *The auditory psychobiology of the mouse* (pp. 201–304). Springfield, IL: Charles C. Thomas.

Winer, J. A., Saint Marie, R. L., Larue, D. T., & Oliver, D. L. (1996). GABAergic feedforward projections from the inferior colliculus to the medial geniculate body. *Proceedings of the National Academy of Sciences of the United States of America, 93*(15), 8005–8010.

Wynne, B., & Robertson, D. (1997). Somatostatin and substance P-like immunoreactivity in the auditory brainstem of the adult rat. *Journal of Chemical Neuroanatomy, 12*(4), 259–266.

Wynne, B., Harvey, A. R., Robertson, D., & Sirinathsinghji, D. J. (1995). Neurotransmitter and neuromodulator systems of the rat inferior colliculus and auditory brainstem studied by in situ hybridization. *Journal of Chemical Neuroanatomy, 9*(4), 289–300.

Yasui, Y., Nakano, K., Kayahara, T., & Mizuno, N. (1991). Non-dopaminergic projections from the substantia nigra pars lateralis to the inferior colliculus in the rat. *Brain Research, 559*(1), 139–144.

Zhang, H., & Kelly, J. B. (2010). Time dependence of binaural responses in the rat's central nucleus of the inferior colliculus. *Hearing Research, 268*(1-2), 271–280.